71st International Astronautical Congress, The CyberSpace Edition, 12-14 October 2020.

IAC–20–A7.2.11

APIS: Applications and Potentials of Intelligent Swarms for magnetospheric studies

Raj Thilak Rajan *, Shoshana Ben-Maor, Shaziana Kaderali, Calum Turner, Dawn Haken, Gary Paul, Vedant, Catrina Melograna, Antonino Salmeri, Sreekumar V, Johannes Weppler, Yosephine Gumulya, Mohammed Milhim, Riccardo Bunt, Asia Bulgarini, Maurice Marnat, Kadri Bussov, Frederick Pringle, Jusha Ma, Rushanka Amrutkar, Miguel Coto, Jiang He, Zijian Shi, Shahd-Lilly Hayder, Dina Saad Fayez Jaber, Junchao Zuo, Mohammad Alsukour, Cécile Renaud, Matthew Christie, Neta Engad, Yu Lian, Jie Wen, Ruth McAvinia, Andrew Simon-Butler, Anh Nguyen, Jacob Cohen

International Space University (ISU), 1, rue Jean-Dominique Cassini 67400 Illkirch-Graffenstaden, France
* Corresponding Author: r.t.rajan@tudelft.nl

Earth's magnetosphere is vital for today's technologically dependent society. The energy transferred from the solar wind to the magnetosphere triggers electromagnetic storms on Earth, knocking out power grids and infrastructure — e.g., communication and navigation systems. Despite occurring on our astrophysical doorstep, numerous physical processes connecting the solar wind and our magnetosphere remain poorly understood. To date, over a dozen science missions have flown to study the magnetosphere, and many more design studies have been conducted. However, the majority of these solutions relied on large monolithic satellites, which limited the spatial resolution of these investigations, in addition to the technological limitations of the past. To counter these limitations, we propose the use of a satellite swarm, carrying numerous payloads for magnetospheric measurements. Our mission is named APIS — Applications and Potentials of Intelligent Swarms.

The APIS mission aims to characterize fundamental plasma processes in the magnetosphere and measure the effect of the solar wind on our magnetosphere. We propose a swarm of 40 CubeSats in two highly-elliptical orbits around the Earth, which perform radio tomography in the magnetotail at 8–12 Earth Radii (R_E) downstream, and the subsolar magnetosphere at 8–12 R_E upstream. These maps will be made at both low-resolutions (at 0.5 R_E, 5 seconds cadence) and high-resolutions (at 0.025 R_E, 2 seconds cadence). In addition, in-situ measurements of the magnetic and electric fields, and plasma density will be performed by on-board instruments. In this publication, we present a design study of the APIS mission, which includes the mission design, navigation, communication, processing, power systems, propulsion and other critical satellite subsystems. The science requirements of the APIS mission levy stringent system requirements, which are addressed using Commercial Off-the-Shelf (COTS) technologies. We show the feasibility of the APIS mission using COTS technologies using preliminary link, power, and mass budgets. In addition to the technological study, we also investigated the legal considerations of the APIS mission.

The APIS mission design study was part of the International Space University Space Studies Program in 2019 (ISU-SSP19) Next Generation Space Systems: Swarms Team Project. The authors of this publication are the participants of this 9-week project, in addition to the Chairs and Support staff.

Keywords: Satellite swarms, Low earth orbit, Heliophysics, Cubesats, Space technology, Autonomous agents

Table of contents

1. Introduction

The heliosphere refers to the area of space under the direct influence of the Sun, which extends from the stellar surface to the outer edges of the solar system. As a space-faring species, we can physically explore this region with satellites, and thereby experimentally test our understanding of heliophysics [1]. This places heliophysics in a privileged position, as only few other branches of astrophysics can lend themselves to in-situ experimentation, and no other branches impact day-to-day life so profoundly. Heliophysics governs the processes occurring around the stars strewn throughout the universe, and we are in the fortunate position of having a natural laboratory to study these processes close to home. The dominant force in the heliosphere is the solar wind — the fast-moving, hot and tenuous stream of charged particles constantly emanating from the Sun [2]. When the solar wind encounters a planetary magnetic field, it flows around the obstacle like water around a rock [1]. Astronomers have observed the collision and interaction of the solar wind and planetary magnetic fields across the solar system, from Mercury's weak magnetic field to the impressive aurorae on Jupiter and Saturn [3–5]. Closer to home, the interaction between the solar wind and Earth's magnetic field sculpts a structure known as the magnetosphere, within which Earth's magnetic field is the dominant force [1]. Figure 1 illustrates this concept and shows the structure of Earth's magnetosphere.

1.1 *Motivation*

Despite occurring on our astrophysical doorstep, some key physical processes connecting the solar wind and the magnetosphere remain poorly understood [1], motivating a steady stream of ongoing research. Understanding the magnetosphere is not only scientifically interesting, but also vital for today's technologically dependent society. Energy transferred from the solar wind to the magnetosphere triggers electromagnetic storms on Earth, knocking out power grids and infrastructure such as communication networks, navigation, and transport. The effects of these geomagnetic storms on spacecraft can be disastrous

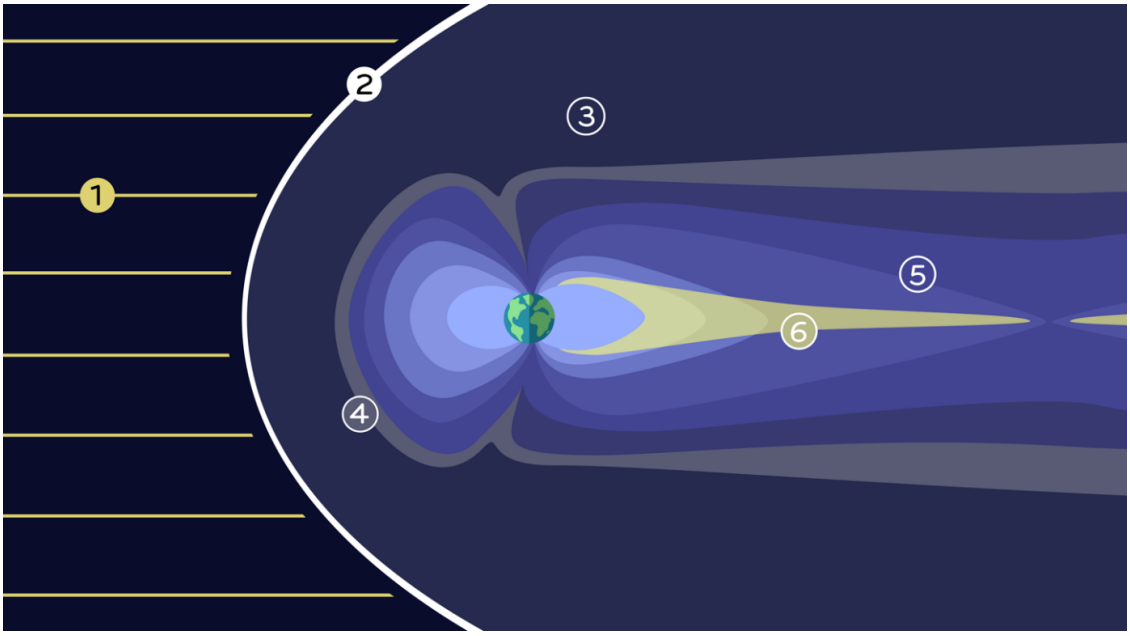

Fig. 1: **The structure of Earth's magnetosphere:** Earth's magnetosphere is shaped by the pressure of the solar wind (1) — a torrent of charged particles that our Sun ejects outwards to interplanetary space. The solar wind interacts with Earth's internally generated magnetic field, which decelerates at the bow shock (2), forming a shock wave. The boundary region at which the pressure of the solar wind is equivalent to Earth's compressed upstream magnetic field is called the magnetopause (4). This region is nearly impenetrable and is located between geosynchronous orbit and the orbit of the Moon. The boundary layer between the plasma bow shock and the magnetopause is the magnetosheath (3) — a transitional region where the density of particles significantly reduces compared to the bow shock. Trapped electrons form two further structures, the inner and outer Van Allen radiation belts. The complex internal structure of the magnetosphere evolves depending on factors such as solar activity. The open magnetic field lines connect to Earth's polar caps where energetic electrons or protons contribute to aurorae. The magnetic field lines carried by the solar wind sweep in to the magnetotail (5) — the teardrop shaped tail of the illustrated magnetosphere. Within the magnetotail, a dense plasma sheet (6) separates the magnetotail's North and South lobes near the equatorial plane. The APIS mission would investigate both the magnetotail and the Sun-ward magnetosphere, with a particular focus on radio tomography in the magnetotail (5).

[6]. Given these practical and scientific motivations, understanding magnetospheric interactions and processes has been a driving requirement for decades of space science missions. There has been a plethora of studies and missions in the past to measure and study a variety of processes in our magnetosphere. However, despite the numerous heliophysics missions that have flown, plasma turbulence and the formation of plasma structures are still elusive and can only be understood with large-scale multi-point measurements. To achieve this goal, we propose the APIS mission (Applications and Potentials of Intelligent Swarms for magnetospheric studies) — which is a swarm of 40 autonomous CubeSats in two highly-elliptical orbits around the Earth, which perform radio tomography in the magnetotail at 8–12 Earth Radii (R_E) downstream, and the subsolar magnetosphere at 8–12 R_E upstream. These maps will be made at both low-resolutions (at 0.5 R_E, 5 seconds cadence) and high-resolutions (at 0.025 R_E, 2 seconds cadence).

1.2 *Outline*

We begin our study with an overview of previous missions, and case studies in Section 2, which includes the key science drivers for the APIS mission and the mission concept. The detailed mission design and mission operations are presented in Section 4 and Section 5 respectively. The APIS satellites

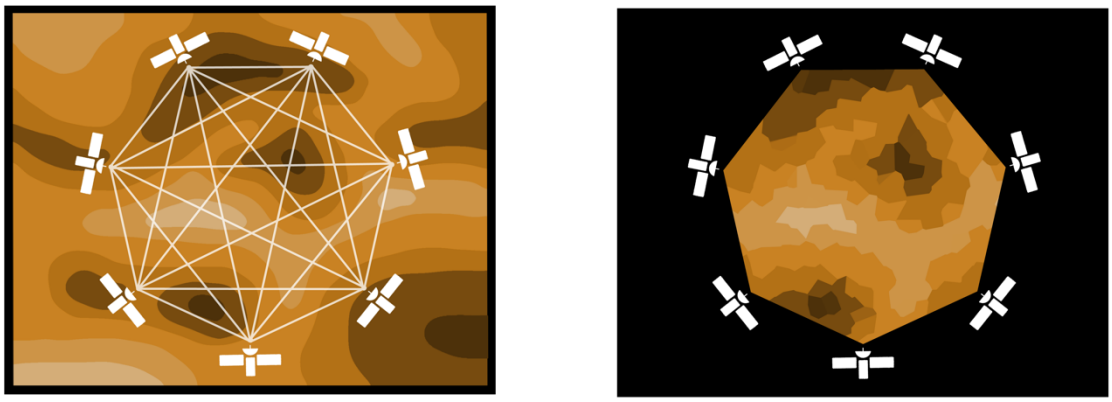

Fig. 2: **Simplified tomography sketch**: Tomography is the process of imaging with the use of penetrating waves. Waves are transmitted along many intersecting lines of sight through a region of interest. The density integral along each of these lines is then derived from the delay in transmission. With many of these line integrals, an estimate of the density map of the region can be produced. This figure shows a simple representation of this process, with the leftmost image showing some field density and the intersecting lines used to measure it. The rightmost figure shows the tomographic reconstruction of the density field within the measured region.

will comprise of various science payloads, which are described in Section 6. Navigation, communication and on-board processing are critical aspects of the APIS swarm, which are addressed in Section 7, Section 8 and Section 9 respectively. The other critical sub-systems including power and propulsion are discussed in Section 10. We briefly address the legal and procedural aspects of the APIS mission in Section 11, and summarize our findings in Section 12.

2. Overview of missions and studies

2.1 *Previous missions*

In the past decades, more than 20 science missions have flown with the aim of investigating Earth's magnetosphere, and many more mission proposals exist on paper. After decades of single-point measurements, multi-point imaging of the magnetosphere is pivotal to the upcoming heliophysics missions. One notable mission that has gathered distributed in-situ measurements is NASA's ongoing mission, THEMIS [7]. Launched in 2007, the mission originally comprised of five satellites in the magnetotail and has provided over 12 years of data collection to date. The payload addresses the science goal of investigating substorms — magnetic phenomena that release energy and intensify aurorae. Another mission capable of collecting three-dimensional information on Earth's magnetic environment and its interaction with the solar wind is ESA's Cluster mission, launched in 2000 and still operational. The four Cluster satellites flying in a tetrahedral formation probe the interactions of electrons and waves in Earth's magnetic environment [8].

A relevant upcoming CubeSat mission is NASA's CubeSat for Solar Particles (CuSP), which is designed to study solar particles in a three-month mission and to act as a pathfinder for a network of "Space Weather Stations" The mission is planned to launch with the Space Launch System in 2021 and consists of a single $30 \times 20 \times 10$ cm CubeSat in a Sun-pointing, trans-Lunar, heliocentric orbit at 1 AU. CuSP is particularly noteworthy for its miniaturized instruments. On a larger scale, NASA's Magnetospheric Multiscale (MMS) mission provides unprecedented high-time resolution multi-point particle and field measurements [9]. Launched in 2015, MMS has a highly eccentric orbit and operates in Earth's magnetosphere using four identical spacecraft flying in a tetrahedral formation. MMS deals with the microphysics of magnetic reconnection, energetic particle acceleration, and turbulence, processes that occur in astrophysical plasmas. Additionally, a group of micro-satellites performed simultaneous multi-point measurements of Earth's magnetic field as part of NASA's ST5 (Space Technology 5). This 90-day mis-

sion mission flew in 2006 and tested 10 new technologies to pave the way for future multi-satellite missions such as MMS and THEMIS. Furthermore, ST5 also contributed to an early understanding of the magnetosphere's dynamic nature [10].

2.2 *Case studies*

The science community has recognized for decades the need for satellites to make simultaneous, distributed heliophysics measurements. The distributed architecture of swarm satellites lends itself to high spatio-temporal range measurements [11], making it a promising architecture for such a distributed measurement mission. Two case studies of proposed magnetic constellations provide insights on how the APIS swarm will perform a next generation heliophysics mission. The case study missions are NASA's MagCon and MagCat, both of which were designed to probe Earth's plasma-sheet and magnetotail. NASA planned these missions to determine how the magnetosphere stores, processes, and releases energy in the magnetotail and accelerates particles to the inner radiation belts. The missions' secondary scientific objective was to study how Earth's magnetosphere responds to variable solar wind and how this influences the magnetopause, the boundary between the solar wind and Earth's magnetic field. Neither mission proceeded further than a concept due to budget constraints.

The Magnetospheric Constellation (MagCon): The proposed Magnetospheric Constellation mission was designed to perform distributed in-situ measurements of the magnetic field, plasma, and particles in such a way as to *"revolutionize our understanding of the magnetospheric response to dynamic solar wind input and the linkages across systems"* [12]. The mission concept was a constellation of up to 36 small satellites weighing 30 kg each with a typical spacing of 1–2 R_E (Earth Radii), using orbits with perigees in the 7–8 R_E range and apogees dispersed uniformly up to 25 R_E [13]. Each spacecraft was designed with a boom-mounted magnetometer and a three-dimensional plasma analyzer to measure Earth's magnetic field. A simple energetic ion-electron particle telescope was also included to analyse charged particle energization, loss, and transport throughout the heliosphere.

The Magnetospheric Constellation and Tomography (MagCat): The Magnetospheric Constellation and Tomography mission was designed to provide the first global images of the magnetosphere [14]. The mission was designed to examine plasma plumes in the magnetosphere, acquire reconstructed images of plasma density and turbulence using radio tomography, and measure three-dimensional ion and electron distributions. Tomography, which gives maps of plasma density [15], is a key facet of the APIS mission.

3. Science drivers for APIS

The aforementioned missions and studies have significantly improved our understanding of small-scale physical processes in the magnetosphere, such as magnetic reconnection and plasma currents [16]. In 2004, NASA stated that MagCon's database of dispersed measurements would allow us to *"emerge from a long and frustrating hiatus"* [17]. Despite the numerous heliophysics missions that have flown, plasma turbulence and the formation of plasma structures are still elusive and can only be understood with large-scale multi-point measurements [13, 18].

3.1 *Motivation*

The APIS mission aims to use a suite of instruments to bridge this gap by providing large-scale maps of plasma density and turbulence in the magnetotail — a need that was identified as early as 2000 [19]. The swarm architecture will allow the temporal and spatial resolution of the tomographic maps to vary over the mission. By providing these high-resolution maps, the APIS mission will address two of the four key science goals set out in the 2013 decadal survey on heliophysics [13]. The baseline tomography measurements meet the spatial resolution (0.5 R_E), and cadence (15 seconds) targets set out by the decadal survey, and the high-resolution operational modes comfortably exceed both of these targets. Based on the decadal survey and past, current, and future heliophysics mission, the APIS mission has two main scientific goals:

- **Goal 1: Discover and Characterize Fundamental Plasma Processes in the Magnetosphere.** The APIS mission should measure the plasma flows and turbulence in the magnetotail using radio tomography and in-situ measurements. The use of a swarm architecture to produce high-resolution, small-scale tomographic maps as well as large-scale observations will help explain key plasma processes that occur, not only in the magnetosphere, but also in magnetized plasmas across the universe [1]. These processes, such as turbulence in a magnetized plasma, require multi-scale multi-point

measurements to be fully understood [18].

- **Goal 2: Determine the Dynamics and Coupling of Earth's Magnetosphere and the Response to Solar Inputs.** The operational architecture of the APIS mission must allow simultaneous plasma density measurements of both the magnetotail and the Sun-facing magnetosphere. The data provided by the APIS mission will uncover couplings in plasma density between different parts of the magnetosphere. Our orbital design would allow for detailed multi-plane measurements of plasma density in the magnetotail, providing long-awaited data to the heliophysics community at unprecedented spatial and temporal resolutions [19]. This data will provide an insight into the plasma dynamics of the magnetosphere in response to solar variation.

3.2 *Regions of interest*

The APIS mission will provide measurements in two initial regions of interest by launching two groups of swarm satellites. The two regions of interests will be in: 1) A near-equatorial orbit in the magnetotail, and 2) A polar orbit that sweeps through the magnetotail and the Sun-ward magnetosphere, over the course of one year. The region of interest for both orbits is 8–12 R_E from Earth, where a host of scientifically interesting processes occur. After creating large-scale tomographic maps, the satellite swarm will then move on to the second phase of science operations and produce high-resolution maps of selected areas within the magnetotail.

The Magnetotail: One group of satellite swarms will be placed in a highly eccentric polar orbit, travelling through the magnetotail — the teardrop shaped tail of the magnetosphere streaming away from the Sun shown in Figure 1. Our region of interest is 8–12 R_E, where key physical processes such as magnetospheric instabilities, plasma flows, morphological changes associated with geomagnetic storms, and turbulence occur [16, 18, 19]. Thus, this region has been intensely studied by previous missions, although at smaller spatial scales than we propose. Initial science observations will provide the big-picture data required to understand the region and the processes happening in this region. The high-resolution follow-up observations will then study these processes in more detail.

Polar plane: A secondary plane of the APIS mission swarm satellites will orbit on the same scale (8–12 R_E), nearly perpendicular to the first plane. This plane will sweep through the magnetotail and the Sunward magnetosphere over the course of a year. While in the magnetotail, the group of satellites in the polar plane will be able to enhance downstream measurements by increasing the region of focus. While in the sub-solar magnetosphere, the swarm satellites will be able to measure Sun-side dynamics. The measurements of plasma densities both up- and downstream of Earth will uncover couplings and dynamics in Earth's magnetosphere.

3.3 *Science measurements*

It is currently not possible to directly image the large-scale plasma structure in the magnetotail. In-situ measurements require an extremely high number of satellites to achieve the desired resolution. Therefore, we propose to use radio tomography to reconstruct the spatial distribution of plasma. Tomography is the process of imaging with the use of penetrating radio waves. The radio waves are transmitted along many intersecting lines of sight through a region of interest. The density integral along each of these lines is derived from the delay in transmission. With many of these line integrals, an estimate of the density map of the region can be produced, as shown in Figure 2. Tomographic methods are well-developed for medical imaging, with examples including Computed Tomography (CT) scanning and medical ultrasound. Thus, the APIS mission will use radio tomography to create estimates of the plasma density in the magnetotail. Radio signals are to be transmitted between the satellites and the time delay of each signal is to be measured. The time delay of the signals is directly related to the total plasma density along the line-of-sight, and a map of the plasma density can then be reconstructed by mathematically combining the line-of-sight density measurements.

The study of the magnetosphere using spacecraft has been proposed [19] and tested [15]. Outside the magnetosphere, International Sun-Earth Explorers 1 and 2 have demonstrated the ability to derive the electron density in the solar wind through radio wave propagation [20]. With measurements between multiple spacecraft, the APIS mission will be capable of investigating the large-scale plasma density structure.

3.4 *Science requirements*

The primary region of interest for the mission is the magnetotail, in the range of 8–12 R_E from Earth. Given the technological limitations of radio transmission, radio propagation measurements with an acceptable Signal-to-Noise Ratio (SNR) cannot feasibly be made across such large distances. Therefore, we

focus on the region of interest defined above. This region contains a sufficiently significant plasma structure to meet the scientific goals. The desired resolution of the tomographic reconstruction is 0.5 R_E. Given the desired resolution of the resultant tomographic image, R_S, and the effective diameter of the area of interest, d the approximate number of linear integrations required is: $N > \pi d/R_S$. The orbital characteristics and the number of spacecraft must meet this driving science requirement. Radio tomography relies on the propagation delay of radio waves in plasma. The APIS mission satellites are to use two basic methods to measure the characteristic delay along a line-of-sight. The first method is known as differential phase [21], which requires two coherent radio signals with different frequencies. The phase velocity of a radio signal in a plasma depends on the frequency and the plasma density. The phase of a probing frequency is compared to the phase of a reference frequency transmitted through the plasma. The resulting phase delay depends on the plasma density as follows:

$$\Delta\phi_1 = \left(\frac{\omega_1 e^2}{2\varepsilon_0 m_e c}\right)\left(\frac{1}{\omega_1^2} - \frac{1}{\omega_{ref}^2}\right)\int ndL \qquad [1]$$

where, ω_1 is the probing frequency, e is the electron charge, ε_0 is the vacuum permittivity, m_e is the electron mass, ω_{ref} is the reference frequency, and n is the total electron content [19]. If the phase delay is greater than 2π, the second method of delay measurement must be employed. The group delay [22] resolves the phase delay that is proportional to total electron content:

$$\Delta t_g \cong -\frac{e^2}{2\varepsilon_0 m_e c}\left(\frac{1}{\omega_1^2} - \frac{1}{\omega_{ref}^2}\right)\int ndL \qquad [2]$$

where the notation is the same as Equation 1, and $\int ndL$ is directly proportional to the total electron content. By combining the methods of differential phase and group delay, we can derive the total electron content. A long-wavelength probing frequency is desired because both types of delay are inversely proportional to frequency. In-situ measurements of the magnetic field and the plasma density are required to interpret the tomography measurements correctly. The scientific measurements must also be correlated with time and position data to produce a complete picture of the magnetotail environment. Tables 1 and 2 encapsulate the scientific motivation and requirements of the APIS mission, as well as the measurement accuracies required. These requirements are based on the decadal survey and previously proposed missions, which can be feasibly achieved with current technology [13, 16, 19, 23].

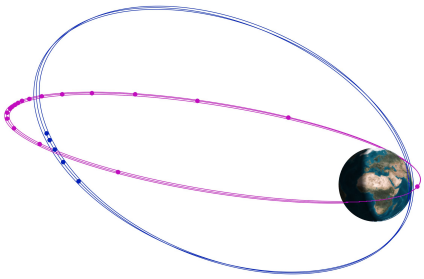

Fig. 3: **Mission Design:** An illustration of the two orbits in the APIS mission — i.e., the Polar orbit (in blue), and the Near-Equatorial (in pink)

.

3.5 *The APIS mission*

The APIS mission will address key physical processes in the magnetosphere, including: how plasma enters the magnetosphere; the formation and dynamics of the plasma sheet; the formation of plasma structures in response to solar wind variability; and turbulence in a magnetized plasma [13]. By exploiting the swarm architecture, the APIS mission will provide large-scale, high-resolution tomographic maps that exceed the targets set out in the 2013 decadal survey on heliophysics [13]. The novel scientific feature of the APIS mission is the swarm-enabled ability to vary the spatial and temporal resolution of the tomography measurements, which will provide the precise data needed to understand key heliophysics processes. The APIS mission requirements, which are discussed at length in the rest of the article, are summarized in Table 3, derived from the science requirements as described in Table 1 and Table 2.

The APIS mission architecture comprises of a homogeneous satellite swarm spread over two orbits, polar and near-equatorial, as illustrated in Figure 3, using the Systems Tool Kit (STK). The swarm satellites will exhibit emergent behavior through cooperation in order to achieve tomography measurements, reference-free calibration of instruments, navigation, and data handling. The presented orbits meet a set of requirements, derived from the science objectives. Table 4 shows the mission orbital parameters, where the Right Ascension of the Ascending Node (RAAN) and the argument of perigee are not mentioned at this time, since the two will depend on the time and date of the launch.

Table 1: Science Requirements for the APIS mission

Requirement	Best Case	Baseline	Minimum
Large-Scale Radio Tomography Phase	Multi-plane tomographic maps of the magnetotail 8–12 R_E downstream, and the subsolar magnetosphere at 8–12 R_E upstream with 0.5 R_E resolution. All measurements at 5 seconds cadence.	Tomographic maps of the magnetotail 8–12 R_E downstream, and the subsolar magnetosphere at 8–12 R_E upstream with 0.5 R_E resolution. All measurements at 10 seconds cadence.	Tomographic maps of the magnetotail 8-12 R_E downstream with 0.5 R_E resolution. All measurements at 15 seconds cadence.
Fine-Scale Radio Tomography Phase	High-resolution tomographic maps of small regions of the magnetotail 8–12 R_E downstream at 0.025 R_E spatial resolution. Measurements at 2 seconds cadence for short bursts.	High-resolution tomographic maps of small regions of the magnetotail 8–12 R_E downstream at 0.05 R_E spatial resolution. Measurements at 3 seconds cadence for short bursts.	High-resolution tomographic maps of small regions of the magnetotail 8–12 R_E downstream at 0.1 R_E spatial resolution. Measurements at 5 seconds cadence for short bursts.
In-situ measurements to anchor tomography	Measurements of: magnetic field, electric field, plasma energy distribution, plasma density; at 2 seconds cadence.	Measurements of: magnetic field, plasma energy distribution, and density; at 3 seconds cadence.	Measurements of magnetic field and plasma density at 5 seconds cadence.
Positional Knowledge	0.01 R_E	0.01 R_E	0.01 R_E
Time Knowledge	0.01 microseconds	0.01 microseconds	0.01 microseconds
Duration of Science Observations	1 Solar cycle (11 years)	2 years	4 months

Over the course of one orbit, the mission operations are subdivided into various phases as illustrated in Figure 4a, which include the science phase and the ground operation phase. The green region indicates the ground link for the mission. Due to the highly eccentric orbit, each satellite will have a window of 1-2 hours per orbit for communication with the ground station. The agents will distribute data amongst the swarm and queue the data in order of importance to the science mission for downlink. The sharing and queuing allows for an effective downlink window of up to 20 hours. The region between the perigee and 8 R_E is dedicated for other functions, such as solar cell charging, orbital maneuvering and attitude control.

The red region in Figure 4a indicates the science phase of the orbit, where the swarm performs tomography and plasma measurements. If one of the satellites recognizes an interesting physical phenomena, the swarm increases the rate of measurements through a consensus decision making process. At the apogee the satellites slow down due to orbital dynamics and the distance between them is reduced to enable better communication between the agents. Therefore, in addition to the science case, the inter-satellite links are also established during this phase, which is critical for swarm-related data processing. Furthermore, individual agents perform science logging preferentially during the ascending phase (agents moving from perigee to apogee), which ensures that inter-satellite data exchange occurs near apogee.

4. Mission design

The objective of the science mission is to map the plasma densities at the scale of 0.5 R_E, for a region of interest from 8 R_E to 12 R_E. To achieve our goal we have designed the swarm to fly in two orbits perpendicular to one another at inclinations of 90° and approximately 0°, with an apogee radius of 14 R_E, enclosing the magnetospheric area of interest. This configuration enables tomography in the magnetotail, as well as in the Sun-ward magnetosphere. In Figure 4b the orbital dynamics that occur during the first year of the mission are illustrated, and the mission phases timeline is described in Table 5.

Table 2: Measurement requirements of the APIS mission (all measurements will have a variable cadence of up to 2 seconds)

Measurement	**Range Accuracy**	**Resolution**
Radio Tomography Plasma Density	0.05–150 cm^3	2 % error acceptable
Magnetic Field	0–2000 nT	0.025 nT
Plasma Particle Energy	1–5 MeV	Energy accurate to 15-20%
In-situ plasma density	0.05–150 cm^3	2% error acceptable

Table 3: APIS mission overview

Mission requirements	
Launcher capability	40 spacecraft (max 24 kg each) deployed in 2 highly elliptical orbits
Mission duration	4 months science phase
Orbital requirement	Apogee of 8–14 R_E, one polar and one near-equatorial plane
Spacecraft requirements	
Attitude Stabilization	3-axis stabilized
Mass	21.8 kg (see Table 13)
Power	63.2 W (see Table 12)
ISL Data Rate	$\geq$ 100 kbit/sec
Pointing	$\leq 5^\circ$ accuracy, $\leq 2^\circ$ knowledge

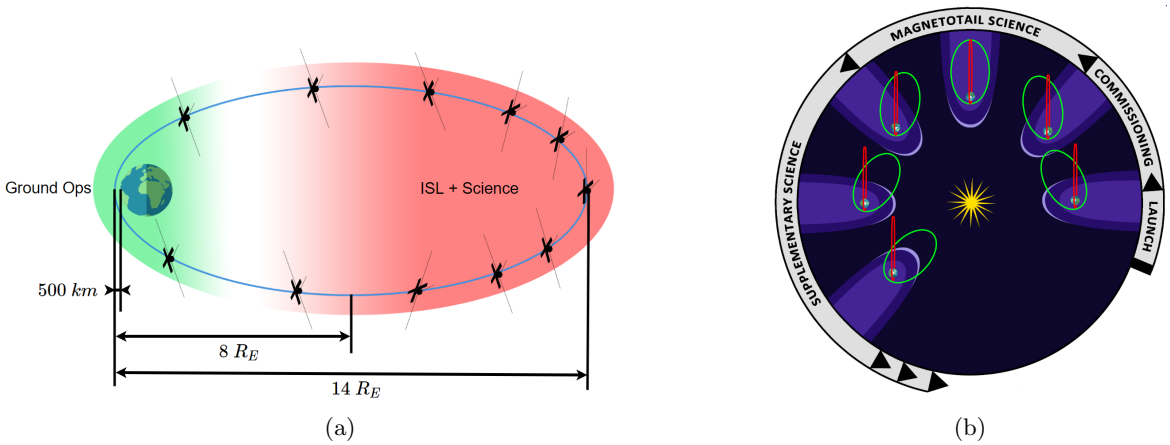

(a) (b)

Fig. 4: **APIS Mission operational phases and configurations:** (a) The 3 phases of the APIS mission are illustrated, over the course of an orbital period for each satellite in the swarm. (b) Illustration of the orbital configuration of the swarm over the course of the one-year mission.

Table 4: Mission orbital parameters

Parameters	**Value**	**Comments**
Apogee	13 R_E (altitude)	14 R_E from the center of Earth in order to enclose the region of interest, defined in by the science objectives.
Perigee	500 km (altitude)	Higher than ISS orbit
Inclination	$\sim 0°$ and $\sim 90°$	One inertially locked in polar, other processes
Number of satellites in each plane	20	Train formation, 18° of angular separation
Eccentric anomaly of the nth satellite	$i\frac{360}{20}n°$	18° of angular separation, n is the satellite number (between 1 and 20)

Table 5: Mission Phases Timeline

Phase	**Description**	**Mission Timeline**	**Duration**
Launch	Launch into highly eccentric orbit	1st day	<1 day
Deployment and commissioning	Swarm agents are deployed at apogee into two possible inclinations (0° or 90°), 20 agents per orbit. Subsystems and payloads are validated and calibrated.	1st day	3 weeks
Science Phase 1	Swarm agents cooperate to perform tomography and plasma property measurements in the magnetotail region.	3rd week	3.5 months
Science Phase 2	Cooperative tomography and plasma measurements in the Sun-ward magnetosphere region are performed on the equatorial orbit, and later on the polar orbit.	6th month	3 months
Science Phase 3	Reconfiguration of swarm agents is executed on both orbits to perform higher resolution tomography in a 2 R_E strip of the magnetotail region	1 year	4 months
Maintenance and Ground Operations	Desaturation of reaction wheels, charging downlink of scientific measurements prioritized by swarm agents, and data analysis.	All mission	
End of life	Passivation of subsystems, natural orbit decay, comprehensive data analysis	Dependent on orbit decay	

4.1 *Nodal precession of the Orbit*

One of the main features of the mission orbit design is the differing nodal precession that occurs between the equatorial and polar orbits, causing the semi-major axis of both orbits to no longer be aligned. Orbital precession affects the orientation of the elliptic trajectory of spacecraft. Nodal precession is defined as the rotation of the orbital plane around the axis of the central body, Earth in our case. This phenomenon is caused by non-uniform mass distribution in the central body, and in a first approximation, the major contributor is the equatorial bulge of Earth, causing the planet to become an oblate spheroid with a larger diameter at the equator than at the poles. The relationship that relates the precession rate to the orbital elements is the following:

$$\omega_p = -\frac{3}{2}\frac{R_E^2}{(a(1-e^2))^2} J_2 \omega \cos(i) \qquad [3]$$

where, a, e, ω and i identify the orbit, R_E is the equatorial Earth radius, and J_2 is the coefficient that takes into account the spherical oblateness of the Earth, as described above. From the two orbits in the APIS mission, only the equatorial orbit is affected by nodal precession. The polar orbit, as characterized by an inclination of 90°, nullifies the precession due to the $cos(i)$ term in the equation given. While the satellites pass through the region of interest and the apogee radius remains between 14 R_E and 8 R_E, where science measurements are to be performed, the experienced

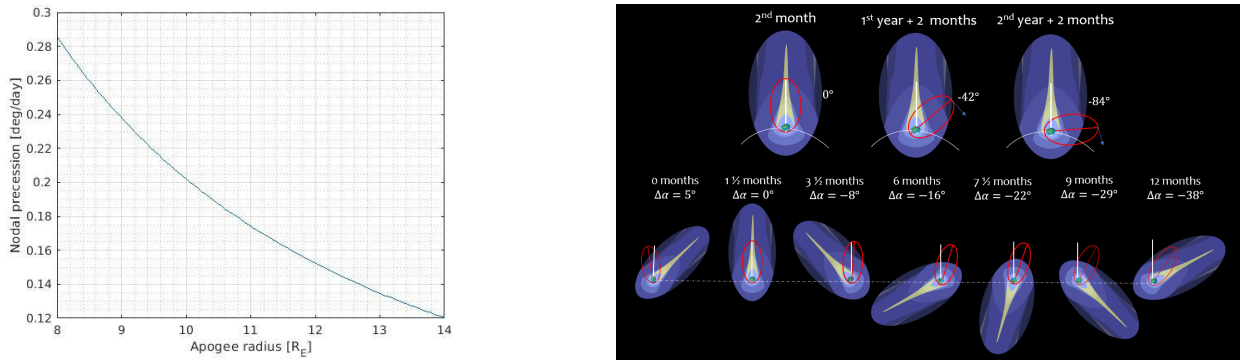

(a) (b)

Fig. 5: **Variation of nodal precession against apogee:** (a) The equatorial orbit used in the mission will experience nodal procession rates of 0.12°–0.29° per day while the apogee radius is 8–14 R_E. (b) Precession of the equatorial orbit relative to the magnetotail.

precession rates will range between 0.12° and 0.29° per day. Figure 5a illustrates how the regression rate varies while the orbit decays in relation to the phases, as illustrated in Figure 5b.

4.2 *Orbital maneuvers*

The minimum science requirement is achieved in the course of the first 3–4 months into the mission, with tomography in the magnetotail. The mission then need an additional two months to perform measurements of the plasma density outside the tail. Following this timeframe, the extended mission will exploit the swarm ability to reconfigure and take new measurements. The objective of the new geometry is to perform higher resolution tomography, as the satellites sweep through the magnetotail in the next orbital pass about 12 months into the mission, which is detailed in Table 5.

Reconfigurability: In the proposed scenario, five satellites from each orbit will perform a maneuver to change their apogee to 2 R_E lower than the reference orbit at 14 R_E. The remaining 30 satellites will stay in their original orbits. The maneuver will take approximately eight months, commencing outside the magentotail and terminating before the satellites sweep through the magnetotail again. Modifying the trajectory of the APIS satellites requires significant thrust due to the high energy of the orbit. To overcome this difficulty, we will use the electric propulsion system on each APIS satellite, which can operate over long periods of time (see Section 10.2). The atmospheric drag experienced during flight close to perigee can also be utilized.

One of the major trade-offs to be considered is the effect of different orbital periods between Group 1 (in the near-equatorial orbit) and Group 2 (in the polar orbit). In Figure 6, the apogee alignment between the two groups is presented, as the orbit decays and the period changes. The two groups are aligned when they reach apogee within one hour of one another.

The swarm is to implement emergent behavior to achieve collaboration between the two orbital groups, thereby improving the potential science return. The desired behavior is to modify the altitudes of both orbits, maximizing the frequency of apogee alignment. This modification will require each satellite to plan the desired attitude at perigee to modulate both the amount of drag experienced and the thrust generated due to turning the propulsion system on and off.

In a first approximation, the electric propulsion system will enable an apogee of 30 km per orbit when used to reduce the velocity in perigee. Attitude control orients the satellites to maximize the satellite surface area exposed to the thin atmosphere. The minimum surface area, used to maintain the 15 satellites in the reference orbit, is 0.06 m^2. The maximum possible area exposing the solar panels is 0.52 m^2, which induces a drag of more than eight times greater than otherwise. Indicatively, the orbit decay, induced by drag on the five satellites moving to the lower orbit, is 20 km per orbit at a perigee altitude of 500 km. A first estimate of the total decay rate induced combining both electric propulsion and drag is in the order of 50 km per orbit.

4.3 *End of mission*

As the swarm decays below the region of interest of 8 R_E, the APIS mission enters the final stage,

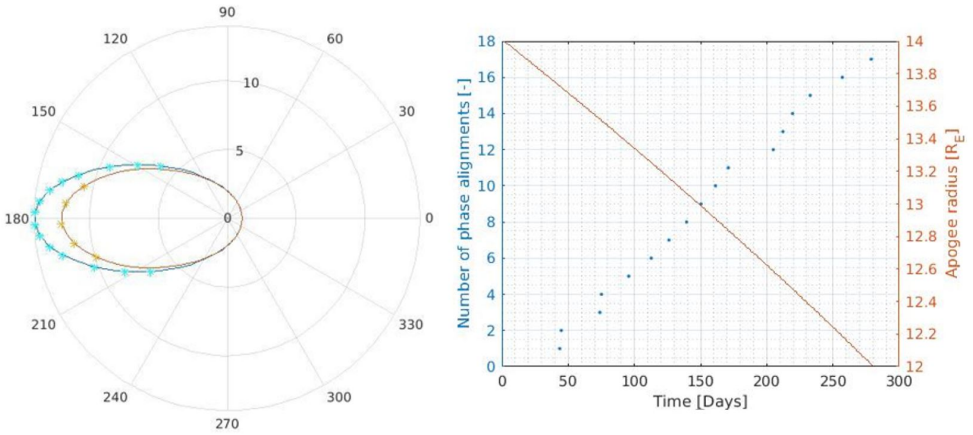

Fig. 6: **Effect of differing orbital periods between groups 1 and 2:** Frequency of apogee alignment between a fixed reference orbit and a reconfigured high resolution orbit is presented.

and no more science is viable. Rapid decay will help minimize the number of spacecraft in orbit. The orbit apogee will decay to a 500 km circular orbit due to the effects of atmospheric drag on the satellites. Once in the circular orbit, the final resources from the propulsion system will be used to lower the perigee and apogee below the ISS. Then the satellites will orbit at the maximum drag attitude orientation while passing through perigee. This procedure will allow for rapid de-orbit, reducing possible intersection with the ISS orbit at lower altitudes.

5. Mission operations

Over the course of the full APIS mission, the satellite swarm will undergo key operational phases. In this section we present an overview of the four mission phases: launch, deployment and commissioning, science, and decommissioning.

5.1 *Launch phase*

Our proposed orbit design outlines a scenario of 40 spacecraft (1040 kg; see Appendix A) distributed over two orbital planes. The difference in inclination between the two planes is 90°. In addition to mass, an important requirement for the launcher is its fairing volume. The total volume to be occupied by the APIS satellites is 0.48 m^3. A single launcher will first inject the whole swarm into a highly eccentric equatorial orbit. Then, once in apogee, a kick-stage will provide enough Δv to change the orbital plane for 20 of the 40 satellites from equatorial to polar. Performing the maneuver in apogee will optimize the use of propellant mass. The following equation provides the Δv required:

$$\Delta v = 2v_a \sin\left(\frac{\Delta i}{2}\right) \quad [4]$$

where v_a is the velocity at apogee, and i is the inclination of the orbital plane. For the APIS mission the final stage will impart a Δv of 1.1307 km/s to a payload mass of 520 kg.

The SpaceX Falcon 9 is a launcher that best meets the requirements for the mission in this scenario, considering both cost and capabilities. The block 5 iteration of the rocket is capable of positioning 8300 kg in Geostationary Transfer Orbit (GTO) [24]. It would therefore be possible for the APIS satellites to share the launcher with other missions, thus reducing the cost. Extending the apogee from the geostationary belt to the required orbit will require a further Δv of 820 m/s.

5.2 *Deployment and Commissioning*

All satellites will be attached to an EELV* Secondary Payload Adapter (ESPA) ring, which is an adapter for launching secondary payloads on orbital launch vehicles and has become a *de facto* standard for various spaceflight missions [25–27]. The commissioning phase is automated, and each swarm satellite tests their payload and bus systems. The satellites transmit any anomalies to the ground for further investigation. Due to the swarm capability, the swarm group in one orbital plane can start its science phase without the need to wait for the swarm group in the second plane. Once all satellites are deployed

*Evolved Expendable Launch Vehicle

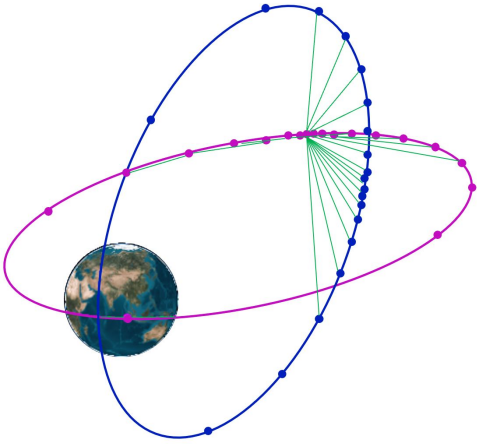

Fig. 7: **Inter-Satellite Link (ISL):** An illustration of ISLs (in green) within the swarm in the APIS mission.

and commissioned in both orbital planes, the science phase will generate results at a significantly higher rate.

5.3 *Science phase*

The majority of the mission's lifetime is the science phase. The orbital design allows the swarm satellites to be in the magnetospheric region of interest by use of orbit precession. The science phase (at an altitude above 50,000 km) lasts for 27 hours per orbit. Tomography techniques require a minimum number of lines to reach the necessary spatial resolution. The swarm will achieve this minimum threshold by performing tomography measurements when close to the apogee area, where due to orbital dynamics, the satellites cluster together at a range of 2 R_E to 8 R_E separation distance . The transmissions will synchronize, using the Code-Division Multiple Access (CDMA) protocol, which leads to the notable swarm behavior. An illustration of these Inter-satellite Links (ISLs) within the swarm is shown in Figure 7.

Each satellite will also perform in-situ measurements of the particle distribution and plasma properties for the tomography data processing. During the 4-month science phase, the satellites will perform 1000 measurement sequences. After each satellite stores its data, the swarm will perform autonomous measurement prioritization based on information theory, which maximizes the scientific return of the swarm. While clustered at apogee, ISL communications are enabled between neighbouring satellites for measurement sharing, data sorting, and autonomous decision-making on measurements to be kept in the collective swarm memory for maximizing the scientific data quality.

5.4 *Decommissioning*

Due to the low-altitude perigee, atmospheric drag is a major perturbation (discussed in detail in Section 4.2), which reduces the orbital eccentricity after every pass. Approximately two years after launch, this slow decay will result in a trajectory designed to plunge the satellite into Earth's atmosphere. This two-year timeline depends on the atmospheric drag experienced by the satellites and on the thickness of the atmosphere, which mainly varies with the solar phase. Using this decommissioning approach offers a sustainable solution to spacecraft failures in the early stages of the mission, while the operating spacecraft will rely on their propulsion systems to maintain the desired orbit. This approach also mitigates for space debris, ensuring that all swarm components will be cleared post mission.

6. Science payloads

All the satellites in the APIS mission comprise of multiple science payloads, including the radio tomography system, and various in-situ measurement systems. In addition, all APIS satellites will employ on-board Radio-Frequency Interference Mitigation (RFIM) techniques and sensor calibration to ensure the veracity of the recorded science data.

6.1 *Radio Tomography*

The APIS mission is to map the plasma density and the electromagnetic field in the Earth's magnetotail to measure the large-scale time-varying structure of the Earth's magnetosphere. Large-scale in-situ measurements of the entire field of interest would require a significant number of satellites, however, with our proposed design, we plan to use radio tomography in order to estimate the plasma density map. In radio tomography imaging, each satellite transmits a coherently phased pair of discrete radio signals, which in turn is received by all satellites. The measured phase difference between the signals, integrated along the ray path, yields the Total Electron Content (TEC). For a network of 15 satellites, with a maximum distance separation of 8 R_E, each satellite-to-satellite transmission and reception takes up to 0.3 seconds, and the entire tomographic cycle takes up to 3 seconds [19]. The choice of the frequency pair — i.e., the probing and reference frequency — plays a vital role in the mission design. For example, in

the MagCat mission (as discussed in Section 2.2), the probing and reference frequencies were of 1 MHz and 3 MHz — i.e., the third harmonic was used [19]. To transmit and receive at these selected wavelengths, a half-wave dipole antenna of approximately 50 m is required, which increases both the mass and power budget of the small satellites.

To overcome power and mass limitations (see Appendix A for detailed tables), the APIS mission plans to use 10 MHz and 30 MHz, as the probing and reference frequencies, respectively. The necessary antenna lengths at these wavelengths is approximately 15 m, which is suitable for the small satellites of the mission. Radio measurements at these selected frequencies can become significantly corrupted by man-made interference [19]. Thus, the APIS mission employs on-board RFIM to resolve this issue. The dual polarized radio signals received by each satellite is to be preprocessed by the Signal Conditioning Unit (SCU), digitized by the Analog to Digital Converter (ADC), and filtered by a Poly-phase Filter Bank (PFB). Finally, the man-made interference is removed by the RFIM block, as illustrated in Figure 8.

The swarm satellites are to deploy two 7.5 m dipole antennas, which will unfurl like measuring tapes. The boom material is a carbon fiber reinforced polymer, while the design is a combination of two arms in the form of 'C'-sections, with one inside the other to reduce volume. Our boom will also act as an insulator, and thus, will be wrapped with aluminized Kapton or another coating to control electrostatic discharge [28].

6.2 *In-situ measurements*

In addition to the radio tomography payload, there are 3 additional payloads on-board the satellites for in-situ measurements.

- *Super-thermal Ion Spectrograph*: The super-thermal ion spectrograph is based on the electrostatic analyzer payload proposed for the CuSP mission [23]. The payload occupies a volume of 1.5U. The payload provides a measure of the energy spectra and the peak intensities of the incident particles, thereby providing in-situ measurements of the magnetospheric plasma.

- *Miniaturized Electron and Ion Telescope*: This payload is based on a flight-proven payload flown on the Compact Radiation Belt Explorer mission in 2018. Our payload will be shielded with tungsten and aluminum, which increases the mass but is necessary to reduce the background noise caused by scattering. The APIS mission miniaturized electron and ion telescope instrument contains a stack of SSDs to image the electron and ion paths. Similar payloads have been flown on-board the ISS [29].

- *Vector Helium Magnetometer*: Vector helium magnetometers have been used in previous missions to measure magnetic fields in various environments. These magnetometers measure the optical properties of helium, which change in an applied magnetic field. Recent and upcoming missions have miniaturized this instrument, and it is now adapted for CubeSat missions like CuSP [23].

6.3 *Calibration*

Calibration is a key challenge for these on-board detectors, especially in long-term missions lasting a few years. Conventionally, operators on Earth correct the errors accrued by the detectors over time via telemetry. As an alternative, the swarm satellites could communicate with each other to employ relative or reference-free calibration, to eliminate the detector errors such as offsets and gain [30]. Since the signal subspace is unknown, the nodes can employ blind calibration [31], which would involve a training phase during the initial deployment of the antennas. Distributed calibration algorithms will be used to ensure the APIS satellite swarm could collectively alleviate their on-board detector errors [32].

7. Navigation

One of the key challenges for the APIS swarm lies in navigation i.e., in ensuring accurate position, time and orientation estimation. A single satellite in the APIS mission has the visibility of GNSS satellites only for a few hours per orbit. In the absence of GNSS, all the satellites rely on their respective on-board Attitude Determination and Control System (ADCS), and the two-way communication with the other satellites in the swarms using Inter-satellite Links (ISLs). In this section, we discuss the clocks and time synchronization, the ADCS system on-board the satellite, and localization strategies with and without GNSS. All the data processing pertaining to the ADCS system will be done by the OBC (Section 9).

7.1 *Clocks and Time synchronization*

The on-board clocks of the satellite swarm in the APIS mission will need to be synchronized for nav-

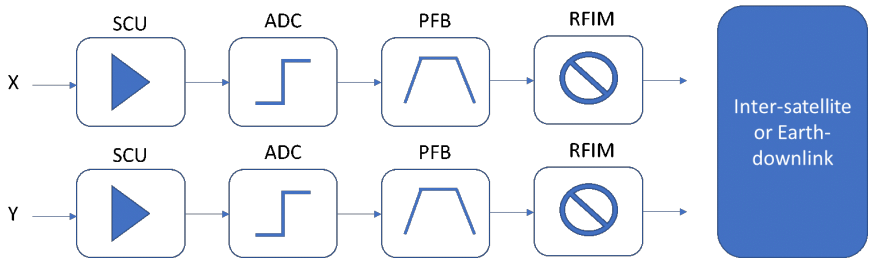

Fig. 8: **Signal processing for RFI mititation:** The block diagram shows a breakdown of the signal processing for radio tomography within a single APIS satellite.

igation, communication, and addressing the science mission [33]. The radio tomography requires accurate transmission and reception at frequencies of 10 MHz and 30 MHz, which is identical to the wavelengths used in interferometry in ultra-long wavelength radio astronomy [34]. The intrinsic stochastic noise on the clock is typically measured in Allan deviation over a coherence time period [35]. The Allan deviation requirements for clocks at these wavelengths are of the order of 10–13, which is typically achieved by oven-controlled crystal oscillators or Rubidium standard clocks [35]. To ensure programmable output frequencies, we propose the use of VCXO Si570, which additionally offers a low-jitter clock output for the range of 0.01–1.4 GHz [36]. The in-depth study of available clocks is beyond the scope of this project.

One of the solutions to align all the on-board clocks within the swarm, is clock synchronization based on time-stamping. Given a time-varying mobile network of satellite swarms, the first-order clock errors, i.e. clock offset and clock drift, can be estimated jointly along with the time-varying distances between the satellites. The satellites will employ two-way ranging to collect the transmitted and received time-stamps. Typically, these measurements are input parameters to optimization algorithms for estimating the unknown clock and distance parameters. In [37], a constrained least squares algorithm is proposed, to estimate these unknown parameters using only time-stamp measurements between the satellites. Furthermore, such algorithms can achieve time synchronization within the network, as long as each satellite has at least one communication link with any other satellite in the network. In addition, a reference for the clock is chosen arbitrarily in the network, and alternatively data-driven references are chosen from the network [37]. The achievable timing accuracy using these algorithms is directly proportional to the bandwidth of communication (i.e. number of time-stamps exchanged), and the SNR of the signals.

7.2 *Attitude Determination and Control System*

The Attitude Determination and Control System (ADCS) in the APIS satellites will comprise of various sensors and actuators to estimate and control the satellite attitude [38]. The chosen components in the ADCS system are COTS components, and have a flight heritage.

- *Reaction wheels*: There are various micro reaction wheels available on the market, which provide a small torque change, and create fine rotations, weighing < 300 g [39]. One of the favourable choices is RWP015 from Blue Canyon Tech, which weighs as low as 130 grams and has a design life of more than five years, and are thus, suitable for the APIS mission [40]. The APIS mission will use the 4-wheel tetrahedron configuration such that in the event of wheel failure the mission can still continue without interruption [38].

- *Magnetic torquers*: In addition to the reaction wheels, magnetic torquers are used for attitude determination using the Earth's magnetic field. The torquers consist of electromagnetic circuits that do not include moving parts, which makes magnetic torquers very reliable and independent of radiation effects as they do not have any sensitive electronics [41]. For the APIS mission, we chose the ISISpace iMTQ Board, which is a PCB-based 3-axis magnetic actuation and control system for 12U CubeSats [42]. It weighs less than 196 grams and is designed as a standalone detumbling system and can also be used with more advanced ADCS hardware, providing actuation of 0.2 Am^2, with a magenetometer accuracy of < 3 μT.

- *Star Trackers*: Star trackers are one of the most accurate sensors for satellite attitude estimation, which is needed during payload operation,

Sun pointing, and for ground link communications. For the APIS mission, we choose the standard NST component from Blue Canyon Tech, which offers an attitude resolution of 6 arcseconds (cross boresight) with a FOV of $10^\circ \times 12^\circ$, and weighs as low as 350 grams [43].

- *Sun Sensors*: In addition to Star trackers, APIS satellites will have Sun sensors on-board to provide orientation information. Sun Sensors are generally less accurate in comparison to star trackers but offer a larger FOV at typically lower costs. There will be four Sun sensors placed in the four selected corners or faces of the satellite body, which is sufficient to provide satellite orientation information with respect to the Sun. The APIS mission will use the two-axis sensor, NFS-NFSS-411, which weighs less than 35 grams, and offers an accuracy of 0.1° with a FOV of 140° [44].

- *Inertial Measurement Unit (IMU)*: IMUs combine accelerometers and gyroscopes, which provide acceleration and orientation information of the satellite, respectively. In particular, MEMS-based IMUs are lightweight and reliable, with longer mission life and offer a high TRL. There are numerous COTS MEMS-based IMUs available in the market — e.g., the Sensonor STIM377H, which is a tactical grade 3-axis IMU comprised of 3 accurate MEMS gyros, 3 high stability accelerometers and 3 inclinometers [45]. Each APIS satellite would have 4 of these IMU units.

7.3 *Relative localization*

In the APIS mission, each satellite will have full access to GNSS signals for only a few hours per orbit. GNSS for navigation will therefore be unsuitable for extended mission duration. The swarm enables collective navigation — i.e., the satellites' relative position to each other can be constantly determined. Huff et al. [46], present a method of obtaining accurate absolute and relative position estimates of a swarm of small unmanned aerial systems. Each APIS satellite will require a GNSS unit, an IMU, and an ISL. When available, GNSS signal measurements will be integrated with the estimated relative positions to determine the absolute position of the satellites. The APIS satellites will use a NovAtel multi-frequency GNSS receiver, OEM719, and the on-board firmware can be reconfigured to offer sub-metre to centimetre positioning, meeting the APIS science requirements of APIS science [47].

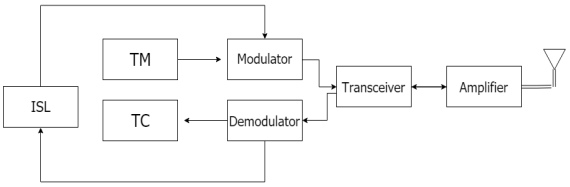

Fig. 9: **ISL communications:** The block diagram illustrates the Inter-satellite link communication system, including the S-band patch antenna, the amplifier, the modulator and demodulator blocks, and the Telemetery (TM) and Telecommand (TC) blocks, which are discussed in Section 8

.

For an immobile network, in the absence of a reference, e.g. GNSS, the relative position of the satellites can be estimated using multi-dimensional scaling like algorithms [48]. Furthermore, [49] proposed a distributed relative position algorithm, which offers a solution to solve for the relative position of satellites cooperatively on a sphere domain. When the satellites are mobile, the relative kinematics (e.g., relative velocity and acceleration) need to be estimated by solving relative kinematics models [50]. A large consideration for the APIS team is distributed control for the swarm in terms of position and attitude. Path-planning feedback control for autonomous and distributed position control of satellite swarms will be implemented, using local sensor data to coordinate individual satellite tasks, with the assumption that each satellite is able to locally process 3D attitude and inter-satellite distances from the on-board sensors. Each satellite can evaluate, in real-time, the final target position based on the available sensor information, and safely navigate to the chosen position while avoiding collision with another satellite. This method of control uses low computational resources and autonomous position selection with safe acquisition, which suit the APIS mission [51].

8. Communication

Communication is a crucial aspect of the APIS mission for autonomy, satellite navigation, and science payload processing. We discuss the Inter-satellite and Earth-based communication in this section. Finally, detailed link budgets for these communication strategies are presented in Appendix B.

8.1 *Inter-satellite link (ISL)*

Individual satellites need inter-satellite links (ISLs) to share information with each other and to transmit the information collected by scientific exploration to the ground center. Thus, the satellites also need satellite-to-ground communication. A simple block diagram in Figure 9 shows the communication system loop for the ISL in the satellite swarm. For the scientific goals of the APIS mission, every satellite must establish a high data rate radio connection with the other satellites, and include a transceiver. The antenna must have sufficient gain and transmission power, and the transceiver must meet the data requirements. According to the existing patch antennas and transceivers available on the market, we investigated five possible antenna systems for the APIS satellites, which are listed in Table 6. Considering the size of the satellite and the data transmission requirements, the S-band patch antenna produced by Endurosat is the chosen antenna for the APIS mission. Along similar lines, we considered four types of transceivers for the APIS mission as shown in Table 7. The transceiver made by ECM Space Technologies GmbH company is attractive in terms of power, volume and mass, which is, therefore, the chosen transceiver for the APIS mission. The ECM transceiver will employ QPSK for transmission and BPSK reception, and offers a data transmission rate of up to 20 Mbps.

8.2 *Uplink and Downlink to Earth*

APIS mission satellites are small in size and restricted in power supply, so at higher orbits the satellites will not be able to communicate directly with the ground-based antennas in full bandwidth. At these orbits, Mobile Ad-Hoc Network (MANET) technology can be used to send information to ground stations. The swarm uses ISLs to hop data from satellite to satellite until the satellite closest to the Earth can send the data to the ground [52]. During Earth fly-by at the perigee, the satellites employ multi-hop communication for data downlink, as illustrated in Figure 10. The MANET system is highly dynamic, fault-resistant, and autonomous, which is advantageous for APIS satellites to communicate data to ground stations. To reduce design complexity, the communications from satellite-to-Earth and ISLs will be combined. Delay Tolerant Networking (DTN) technology will store and transmit data back to ground stations, following processing, once satellite have reached a low-altitude location, providing reliable communication in case of network connection interruption [53].

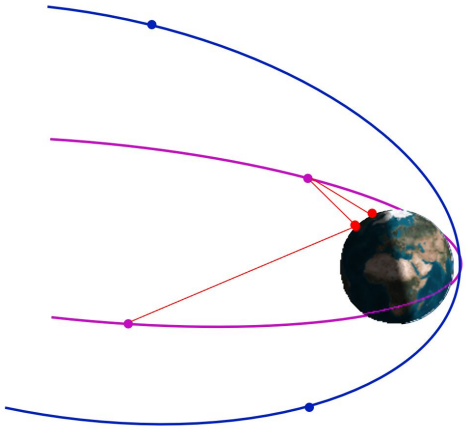

Fig. 10: **Swarm satellite downlink:** Swarm satellites can communicate with ground stations while in the equatorial orbit. Red lines indicate ground link communication with satellites.

Using the THEMIS mission as a reference, we estimate a data rate of up to 500 bytes/second from all of the science payloads [16]. The APIS satellites can have up to 20 Mbit/s of data downlink. To manage thermal issues and data packet loss we assume a guaranteed data rate of 1 Mbit/s. With one hour of contact to the ground station, each satellite can transmit up to 400 MB. Assuming a 50% success rate of package transmission, as commonly used [16], the data transmission per perigee pass reduces to 200 MB. Furthermore, assuming half the data consists of telemetry and housekeeping data, we can then assume a success full transmission of up to 100 MB of science data per perigee pass. A summary of all the communication and operational requirements is listed in Table 8.

9. On-board processing

The On-Board Computer (OBC) is a crucial component to the functionality of the mission and is responsible for reading, collecting, and processing sensor information from the ADCS, GNSS, and communications systems — which includes executing Telemetry, Tracking and Command (TTC) operations, and storing on-board health data. Additionally, the OBC is responsible for maintaining the On-Board Timers (OBT) for synchronization, localization, control, and performing inertial referencing calculations [54]. In addition, the OBC must execute

Table 6: Antenna comparison table

Manufacturers	NanoAvionics	Endurosat	Anywaves	AAC-Clyde Space	Surrey
Website	n-avionecs.com	endurosat.com	anywaves.eu	aac-clyde.space	surreysatellite.com
Operating Frequency (MHz)	2400–2450	2400–2450	2025–2290	2200–2300	2000–250
Gain (dBi)	6	8.3	6.5	7	3
Circularly Polarized	Yes	Yes	Yes	Yes	Yes
Mass (g)	49	64	123	50	80
Dimension (l×w×h mm)	70 × 70 × 12	98 × 98 × 12	79.8 × 79.8 × 12.1	81.5 × 89 × 4.1	82 × 82 × 20

Table 7: Transceiver comparison table

Manufacturer	NanoAvionics	ECM	Spacecom	Skylabs
Website	n-avionecs.com	ecm-space.de	iq-spacecom.com	skylabs.si
Tx. Freq. (MHz)	2200–2290	2200–2290	2200–2290	2200–2300
Rx. Freq. (MHz)	2025–2110	2025–2110	2025–2110	2000–2100
Tx. Bit Rate	128-512 kbps	20 Mbps	20 Mbps	4 Mbps
Modulation	GMSK	QPSK, BPSK	BPSK, QPSK, 8PSK	OQPSK
Output Power (dBm)	30	27	30	30
Power Consumption (W)	5	12	13	5
Mass (g)	190	190	190	90
Dimension (l×w×h mm)	87 × 93 × 17	50 × 55 × 94	50 × 55 × 94	95 × 91 × 10

all expected tasks while abiding to bus requirements. Thus, we need to keep the power consumption and mass low, with the frequency and Total Ionizing Dose (TID) high. Higher frequency ensures tasks can be completed within the lowest necessary time, however, this requires high power consumption. Thus, both frequency and power must be balanced.

Since the APIS mission is to study the magnetosphere outside of LEO, radiation hardening of the OBC processor is an important requirement, as the charged particles ejected from the Sun can cause detrimental and undesired effects to the on-board electronics [55, 56]. Based on the NASA RHESE project, radiation hardening of OBC components is recommended through: material hardening of OBC components and shielding; the inclusion of redundant hardware; software verification and reconfigurability [55]. The measure of accumulated radiation a device can withstand prior to becoming unreliable is known as the TID, which acts as a metric for the life expectancy of the device [56], and sets the parameters for radiation hardening. A higher TID ensures a higher life expectancy for the electronics.

A trade study was completed to compare the available options viable for the APIS mission listed in Table 9. All three options have similar dimensions, though, ISISpace offers the highest operating frequency at the cost of higher power consumption. However, for the APIS mission, mass is a critical criteria, and hence we chose the IMT component, weighing nearly half the mass of the remaining two options.

The satellite swarm in the APIS mission will comprise of autonomous satellites, and to that end will each achieve (a) Self-configuration, (b) Self-optimization, (c) Self-healing and (d) Self-protection, during mission operation [57]. If an autonomous system has the authority to make changes to its command, and behaves in an unexpected way, it will reduce the level of trust between the system and its operators [58]. Changes in trust levels will complicate mission design and may necessitate the creation and installation of safeguards that further increase system complexity. In addition to exploiting autonomy, the APIS mission will facilitate distributed functionality, enabling emergent behavior of the satellite swarm.

To enable the emergent behavior of the swarm satellites, we need to partner an appropriate operating system with the OBC. NASA conducted research

Table 8: Communication and operational requirements

Ground station passes	1 pass every 2 days; 1 hour window
Antenna size	98 × 98 mm
Data volume per pass per satellite	40–400 MB
Uplink and downlink frequency	2.45 GHz
Power available for communication	4 W (average)
Downlink data rate	$\geq$ 20 mbit/sec

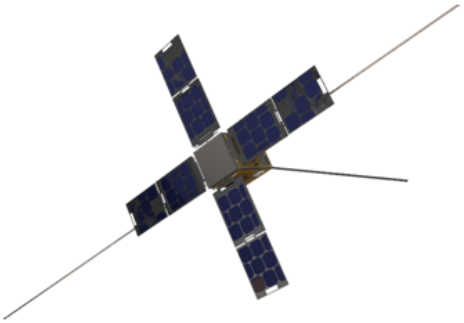

Fig. 11: **APIS satellite solar panels:** An illustration of the solar panels deployed in an APIS satellite. The solar panels are fixed in a windmill fashion to ensure the panels are consistently facing the Sun during orbit, gaining maximal solar energy for powering satellite system.

on the feasibility of using COTS technology for the Command and Data Handling (CDH) system of a swarm of satellites [59]. The study used an android operating system with specific programming to relay data from both satellite-to-satellite and satellite-to-ground stations, demonstrating the feasibility of the satellite swarm behavior using COTS software. We recommend using an adapted version of FreeRTOS, which can process, allocate, and communicate tasks in a large-scale multi-processor network with reduced network congestion and communication energy [60].

10. Satellite systems

In addition to the navigation, communication and on-board processing, the APIS satellite will contain power and propulsion systems. We briefly discussed these subsystems in this section, and give an insight on the APIS satellite structure.

10.1 *Power system*

The electrical power system deals with the generation, storage, monitoring, control, and distribution of electrical power.

- *Generation*: Solar panels are the safest, and cheapest choice for the missions for near-Earth orbit. The state of the art AM0 ATJ (Advanced Triple Junction) or ZQJ (Azur Quad Junction) solar cells available give greater than 35% beginning of life efficiency, and will produce 245 W/m^2 [61]. The battery acts as a backup support whenever the solar cells or array fail to point towards the Sun during maneuvers or payload operations. The satellite does not have a payload pointing requirement. The solar panel is deployable and fixed, instead of variable for sun-tracking. Moreover, body-mounted solar cells cannot meet the power requirements of the satellite swarms, thus, a deployable solar panel is necessary. There are two panels for each side in a fixed configuration, and the solar panel parameters are presented in Table 10 . We have fixed a windmill design of the solar panels such that they are always pointing towards the Sun during their orbit, this design can be viewed in Figure 11.

- *Storage*: Lithium Ion (Li-Ion) cells are reliable in both small and large satellite applications, and their performance can be further enhances with carbon nanotube electrodes [62]. Figure 12 shows the energy balance for the battery, where the estimated charge and discharge cycles are illustrated during mission life. For a five-year mission, a safe limit with a margin for depth of discharge (DoD) of 20% is about 30,000 cycles. With these constraints, we recommend the LG18650MJ1 Li-Ion cell with the battery sizing as listed in Table 11.

- *Power control and monitoring*: Traditionally, the power control unit regulates power from the solar panels and batteries. The power control then consists of three units to adjust the output, and charge the battery pack. A better system would include a digitally integrated array control and battery charging unit [63]. Additionally, the system determines the health of criti-

Table 9: Potential OBC options and specifications

OBC Option	**Power Consumption (mW)**	**Mass (g)**	**Dimensions l × w × h (mm)**	**Frequency (MHz)**	**Total Ionizing Dose (kRad)**
ISIS	400	76	96 × 90 × 12.4	400	N/A
CubeComputer	200	50–70	90 × 96 × 10	48	20
IMT	300	38	96 × 90 × 10	200	15

Table 10: Solar panel parameters

Parameter	**Value**
Face area	0.04 m^2
Generation @ BOL	78.5 W
ATJ/ZQJ 0.5 mA cells in parallel	4
Number of strings	4
Regulation control	IAC-BC
Total Panel Area (2 panels × 4 panels)	0.32 m^2
Generation @ EOL	67 W
Number of cells in series	14
Power loss per string	16 W
Estimated weight	1.4 kg

cal power elements and has a set of protection against overloads, undervoltage, and overvoltage occurrences.

- *Power distribution*: Power distribution systems can be distributed or centralized. The best choice for the APIS satellites are Solid-State Power Controllers (SSPC), as they are more reliable than electromechanical relays and are re-triggerable in case of faults caused by noise, electromagnetic interference or radiation effects [64]. For satellites of 12U size, a centralized, regulated distribution will be efficient in mass and volume with all bus systems powered with a single Direct Current/Direct Current (DC/DC) module. We recommend dedicated DC/DC converters for redundant systems to avoid single-point failures, where one failure could otherwise affect the entire satellite. The payload is sensitive, requiring completely different voltage scales, and should have local DC/DC converters, a low drop-out regulator, and a switch to disconnect the system from the source for isolating a fault if required.

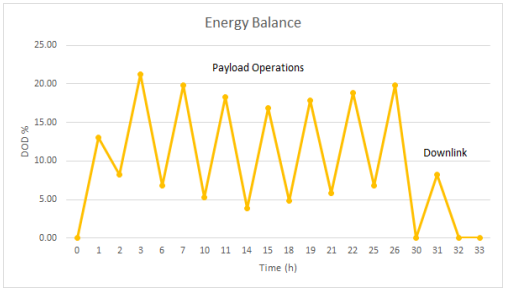

Fig. 12: **APIS satellite energy balance:** The typical energy balance for an APIS satellite battery over the course of one orbit is presented. Charge and discharge cycles need careful consideration in terms of battery life.

10.2 *Propulsion system*

The propulsion system consists of thrusters mainly used for orbital corrections. The satellites in the APIS mission require in-orbit corrections, and therefore, an on-board propulsion system. Two popular solutions include the Pulsed Plasma Thurster (PPT) and the Micro Electrospray Propulsion (MEP). MEPs use the principle of electrostatic extraction and acceleration of ions. The propulsion system does not need gas-phase ionization, which is an advantage. The propellant is not pressurized since it flows through capillary action. The emission is controlled by modulating the voltage applied. This provides better safety in handling the spacecraft and lighter weight [65]. MEPs offer high system-level and power level efficiencies. However, there are severe system scalability issues, thus, making MEPs harder to use.

PPTs are known for having a high specific impulse, consisting of low power electric thrusters for precise spacecraft control, and can be used for orbit maintenance [66]. The thruster uses electricity, to vaporize the solid Teflon propellant to generate thrust. PPTs do not need a tank or feed system, are compact, low-cost, and consume less power in contrast to MEPs. The drawback of a PPT operation is that it

Table 11: Battery Parameters

Parameter	Value
Allowed DoD	<20%
Load power	**Peak:** ∼54 W **Idle:** 34 W
Discharge at average voltage	**Peak:** 10 A (100 ms/3 s) **Nominal:** 1.1 A
Regulation control	IAC-BC
Final battery size	8S4P
Duration	1 h
Number of cells in series	8
Total cycles	∼30 000
Cell	LG18650MJ1 3.5 Ah
Capacity	400 Wh

may create disturbances in payload science measurements because of the possible mixing of propulsion plasma with magnetotail plasma. We can mitigate for this risk with strategic scheduling of propulsion use [67]. The APIS satellites will, therefore, use a variant of PPT called Filament Pulsed Plasma Thruster (FPPT), which uses a Polytetrafluoroethylene propellant [68]. Two propulsion systems will be placed aligned to the center of mass such that the system can be used for both linear and rotational movement. The thruster can also be used as a desaturating unit for the reaction wheels through the on-board computer (OBC).

10.3 *Structures and Thermal*

The structure subsystem is the skeleton that supports all the other subsystems, including the spacecraft frame and deployable solar panel and antenna. We favor the skin-frame structure over a simple frame structure because of its resistance to bending, tensional and axial forces [69], and prefer an aluminum and carbon-fiber-epoxy as the material for our bus. A preliminary study of power, volume, and mass estimates for the science payloads and the various subsystems are listed in A, where an APIS satellite is expected to be a CubeSat, with a possible 12U form factor — i.e., 226 mm × 226 mm × 340 mm. A comprehensive system design, however, is an on-going investigation, and will be presented in subsequent work. In addition, we would like to investigate various thermal control methods including both active and passive systems, suitable for the APIS mission.

11. Legal Requirements and Procedures

APIS is a National Aeronautics and Space Administration (NASA) sponsored mission requiring compliance with United States (US) law, where space activities are regulated by administrative agencies. The NASA Act provides rules and procedures for launch authorization and frequency allocation for NASA missions [70]. NASA also complies with space debris mitigation, registration, and environmental protection regulations [71]. When purchasing parts or contracting services, NASA must comply with the Federal Acquisition Regulation (FAR), although US federal law provides some alternatives that could simplify the process. Certain frequency assignments by the National Telecommunications and Information Administration (NTIA) — in coordination with the Federal Communications Commission (FCC) — are required.

Space activities using radio frequencies require authorization from the International Telecommunication Union (ITU), which is the authority on the international level for management and coordination of the electromagnetic spectrum. Within the ITU system, states apply for frequency spectra to be distributed at the national level between commercial and governmental activities. In the US, while commercial applications for frequencies are managed by the FCC, requests from governmental agencies are handled by the NTIA. Frequency licensing for NASA missions is managed by a spectrum manager [72]. Registration procedures vary depending on national legislation and in the US, each space object launched into outer space is individually registered with the national registry. The UN is also notified.

11.1 *Sustainability*

Space sustainability is the concept that outer space should remain accessible and useful for all humankind into the future [73]; however, the team recognizes that the use of satellite swarms may be contrary to this concept if adequate mitigation plans are not in place. Each NASA mission requires an appropriate orbital debris mitigation plan [71, p. 2]. The UN space debris mitigation guidelines also require an orbital debris limitation plan to account for the safe de-orbit of non-functional space objects. Regarding the risk of collision, the orbital architecture of the APIS mission requires the satellite swarm to periodically pass through LEO, posing a risk of collision with other objects. However, the train formation — i.e. satellites only crossing LEO one at a time and only for a very short period — significantly reduces

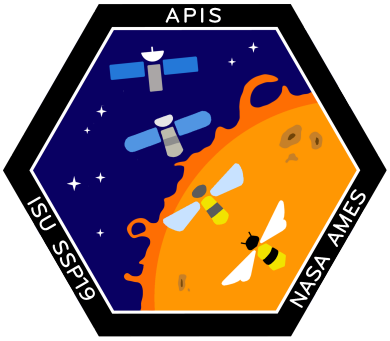

Fig. 13: APIS mission patch

this risk. Indeed, any mission has a chance of failure, and failed satellites may turn into space debris. The mission's low altitude orbit in LEO (about 500 km) ensures that non-functioning satellites will de-orbit within approximately two to three years, well within the current 25-year limit, as discussed in Section 5.4.

12. Conclusion

The APIS mission aims to characterize fundamental plasma processes in Earth's magnetosphere and measure the effect of the solar wind on the magnetosphere. We propose a swarm of 40 CubeSats in two highly-elliptical orbits around the Earth, which would investigate both the magnetotail and the Sunward magnetosphere, with a particular focus on radio tomography in the magnetotail. The APIS satellites will employ radio tomography, and carry various in-situ measurement systems on-board, e.g., Superthermal Ion Spectrograph, Miniaturized Electron and Ion Telescope, and Vector Helium Magnetometer, to provide large-scale maps of plasma density and turbulence in the magnetotail. The minimum science requirement, of radio tomography in the magnetotail is achieved in the course of the first 3–4 months into the mission. At the end of 1 year, all the key science phases are completed. Towards the satellite design, various subsystems have been investigated in depth, which includes the navigation, communication, onboard processing, power and propulsion systems. We show that COTS technologies available today can be used to meet the outlined science requirements. APIS is a NASA funded project, and hence would comply with US regulations, which is also briefly investigated.

A preliminary investigation on the power, mass and volume budget of a single satellite indicates that the APIS mission could be designed using homogeneous CubeSats (Appendix A), with a possible 12U form factor (226 mm × 226 mm × 340 mm). However, a comprehensive system design needs further study. In addition to a detailed system model, some of the key future challenges include distributed algorithms for swarm behaviour, including energy-efficient communication [74], smart autonomous navigation [75], distributed processing [76], attitude control [77], and in-depth mission planning [78, 79]. Furthermore, significant advances in propulsion technology [80], and miniaturization of satellite subsystems and payloads in the upcoming decades will yield smaller satellites and larger swarms, subsequently benefiting the APIS mission [51].

12.1 *Acknowledgement*

The APIS mission design study was part of the International Space University Space Studies Program in 2019 (ISU-SSP19) as the Next Generation Space Systems: Swarms Team Project, which is partially funded by NASA. This 9-week intense project was conducted by a team of 32 members from 16 nationalities, who are drawn from diverse professional backgrounds, ranging from engineers and scientists to lawyers and managers from the space sector. The authors of this publication include the APIS team, the Chairs Dr. Jacob Cohen, Anh Nguyen and Andrew Simon-Butler, and the support staff Ruth McAvinia. The name of the project is adopted from the genus name *Apis*, meaning 'Bee' in Latin, which was an inspiration for the APIS mission patch designed during this study. See Figure 13.

Table 12: Preliminary power budget

System	Average (W)	Idle (W)	Peak (W)
Payload	10	1	250
DHS	2	2	2
IMU	2.4	2.4	2.4
RF/ISL Link	13	1.7	38
AOCS/OBC	10	10	10
Reaction Wheels	2.4	2.4	4
Magnetic Torquers	0.175	0.175	1.2
Propulsion	0	0	48
Thermal	8	5	15
Power Electronics	4	4	4
Battery Charge	10	5	20
2% Losses	1.2395	0.6735	7.892
Total Load:	**63.2**	**34.3**	**N/A**

A. Power and Mass budgets

In this section, a preliminary power and mass budget of an APIS satellite is presented, using the chosen COTS components for various science payloads and satellite subsystems. These budgets are not comprehensive, but give an indication of the size, mass and power consumption of the designed satellite. Table 12 shows the power budget, which can be met by the proposed on-board power system (see Section 10.1). Table 13 includes the mass and dimensions of a single APIS satellite, leading to a total mass of less than 24 Kg. Given the dimensions of the various APIS subsystems, the APIS satellite will be a CubeSat, with a possible 12U form factor (226 mm × 226 mm × 340 mm). However, the entire system design is an ongoing investigation.

B. Communication link budgets

In this section, we present the communication link budgets for an APIS satellite. Table 14, Table 15 and Table 16 show the Downlink, Uplink and Inter-satellite Link (ISL) budgets respectively.

Table 13: Preliminary mass budget

System	Component	Mass (kg)	Dimension (mm)
Payload	Ion Sensor	1.37	100 × 100 × 150
	Vector Helium Magnetometer	0.82	100 × 100 × 50
	Mini Electron ion Telescope	1.1	100 × 100 × 90
	Tomography Electronics	1	100 × 100 × 20
	Tomography Antenna (stowed)	1	15 000 × 27
	Tomography Antenna (deployed)		90 × 90 × 40
	Magnetic Boom	0.4	8 x 680
C&DH	OBC	0.5	96 x 90 x 17
ADCS	Reaction Wheels (4)	0.52	46 × 46 × 19
	Torquers (4)	0.8	96 × 90 × 17
	Star Tracker (1)	0.36	100 × 55 × 50
	Sun Sensor (4)	0.14	34 × 32 × 20
	IMU (4)	0.22	39 × 45 × 22
GNSS	Receiver	0.1	71 × 46 × 11
	Antenna	0.1	N/A
Structure	Frame (e.g.,12U)	1.5	226 × 226 × 340
Communications	S-Band Antenna	0.07	98 × 98 × 12
	Amplifier	0.3	68 × 45 × 12
	Transceiver	0.1	95 × 50 × 55
Power System	Solar Panel (8)	1.4	200 × 200
	Battery	1.80	96 × 96 × 144
	Electronics	0.5	80 × 80 × 70
Thermal System	Thermal Control	1.5	N/A
Propulsion	Propellant	1.2	96 × 96 × 96
	Dry Mass	4	N/A
Misc.	Harness	1	N/A
	Total:	**21.8 kg**	

References

[1] C. J. Schrijver and G. L. Siscoe, *Heliophysics: Plasma Physics of the Local Cosmos*, C. J. Schrijver and G. L. Siscoe, Eds. Cambridge: Cambridge University Press, 2009. [Online]. Available: http://ebooks.cambridge.org/ref/id/CBO9781107340657

[2] M. Kivelson, M. Kivelson, and C. Russell, *Introduction to Space Physics*, ser. Cambridge atmospheric and space science series. Cambridge University Press, 1995. [Online]. Available: https://books.google.nl/books?id=qWHSqXGfsfQC

[3] B. A. Smith, L. A. Soderblom, T. V. Johnson, A. P. Ingersoll, S. A. Collins, E. M. Shoemaker, G. E. Hunt, H. Masursky, M. H. Carr, M. E. Davies, A. F. Cook, J. Boyce, G. E. Danielson, T. Owen, C. Sagan, R. F. Beebe, J. Veverka, R. G. Strom, J. F. McCauley, D. Morrison, G. A. Briggs, and V. E. Suomi, "The Jupiter system through the eyes of Voyager 1," *Science*, vol. 204, no. 4396, pp. 951–972, 1979.

Table 14: Downlink budget

Downlink Frequency:	**2150 MHz**
Distance:	**18846.8 km**
Spacecraft:	
Spacecraft Transmitter Power Output:	8.0 W
	9.0 dBW
	39.0 dBm
Spacecraft Transmission Line Losses:	-1.0 dB
S/C Connector, Filter or In-Line Switch Losses:	0.0 dB
Spacecraft Antenna Gain:	8.3 dBiC
Spacecraft EIRP:	46.3 dBm
Downlink Path:	
Spacecraft Antenna Pointing Loss:	-1.0 dB
Antenna Polarization Loss:	-1.5 dB
Path Loss:	-184.6 dB
Atmospheric Loss:	-2.2 dB
Isotropic Signal Level at Ground Station:	-143.2 dBm
Ground Station:	
Ground Station Antenna Pointing Loss:	-2.0 dB
Ground Station Antenna Gain:	31.35 dBiC
Ground Station Transmission Line Losses:	-1 dB
G.S. Transmission Line Coefficient:	0.7943
Ground Station Effective Noise Temperature:	542 K
Ground Station Figure of Merit (G/T):	3.0 dB/K
G.S. Signal-to-Noise Power Density (S/No):	86.4 dBHz
System Desired Data Rate:	2.00×10^7 bps
	73.0 dBHz
Telemetry System Required Eb/No:	10 dB
System Link Margin:	**3.4 dB**

Table 15: Uplink budget

Uplink Frequency:	**2150 MHz**
Distance:	**35040.5 km**
Ground Station:	
Transmitter Power Output:	50.0 W
	17.0 dBW
	47.0 dBm
Transmission Line Losses:	-3.0 dB
S/C Connector, Filter or In-Line Switch Losses:	-1.0 dB
Antenna Gain:	31.4 dBiC
Ground Station EIRP:	74.3 dBW
Uplink Path:	
Ground Station Antenna Pointing Loss:	-1.0 dB
Antenna Polarization Losses:	-4.0 dB
Path Loss:	-190.0 dB
Atmospheric Losses:	-3 dB
Isotropic Signal Level at Ground Station:	-124.7 dBm
Spacecraft:	
Spacecraft Antenna Pointing Loss:	0.0 dB
Spacecraft Antenna Gain:	8.3 dBiC
Spacecraft Transmission Line Losses:	-1 dB
S/C Transmission Line Coefficient:	0.7943
Spacecraft Effective Noise Temperature:	250 K
Spacecraft Figure of Merit (G/T):	-16.7 dB/K
S/C Signal-to-Noise Power Density (S/No):	87.3 dBHz
System Desired Data Rate:	2.00×10^7 bps
	73.0 dBHz
Telemetry System Required Eb/No:	10 dB
System Link Margin:	**4.2 dB**

[4] J. T. Clarke, J. Nichols, J. C. Gérard, D. Grodent, K. C. Hansen, W. Kurth, G. R. Gladstone, J. Duval, S. Wannawichian, E. Bunce, S. W. Cowley, F. Crary, M. Dougherty, L. Lamy, D. Mitchell, W. Pryor, K. Retherford, T. Stallard, B. Zieger, P. Zarka, and B. Cecconi, "Response of Jupiter's and Saturn's auroral activity to the solar wind," *Journal of Geophysical Research: Space Physics*, vol. 114, no. 5, pp. 1–20, 2009.

[5] R. M. Winslow, B. J. Anderson, C. L. Johnson, J. A. Slavin, H. Korth, M. E. Purucker, D. N. Baker, and S. C. Solomon, "Mercury's magnetopause and bow shock from MESSENGER Magnetometer observations," *Journal of Geophysical Research: Space Physics*, vol. 118, no. 5, pp. 2213–2227, 2013.

[6] J. N. Pelton and F. Allahdadi, Eds., *Handbook of Cosmic Hazards and Planetary Defense*. Cham: Springer International Publishing, 2015. [Online]. Available: http://link.springer.com/10.1007/978-3-319-03952-7

[7] V. Angelopoulos, "The THEMIS mission," *Space Science Reviews*, vol. 141, no. 1-4, pp. 5–34, 2008.

[8] C. Escoubet, M. Fehringer, and M. Goldstein, "The cluster mission," *Annales Geophysicae*, vol. 19, pp. 1197–1200, 09 2001.

[9] T. Karlsson, F. Plaschke, H. Hietala, M. Archer, X. Blanco-Cano, P. Kajdič, P. A. Lindqvist, G. Marklund, and D. J. Gershman, "Investigating the anatomy of magnetosheath jets - MMS observations," *Annales Geophysicae*, vol. 36, no. 2, pp. 655–677, 2018.

[10] R. M. Young, "Updated heliostorm warning mission: Enhancements based on new technology," *Collection of Technical Papers*

Table 16: Inter-Satellite link budget

ISL Frequency:	**2150 MHz**
Distance:	**35040.5 km**
1st Spacecraft:	
Spacecraft Transmitter Power Output:	8.0 W
	9.0 dBW
	39.0 dBm
Spacecraft Transmission Line Losses:	-1.0 dB
S/C Connector, Filter or In-Line Switch Losses:	0.0 dB
Spacecraft Antenna Gain:	8.3 dBiC
Spacecraft EIRP:	46.3 dBm
Crosslink Path:	
Spacecraft Antenna Pointing Loss:	-1.0 dB
Antenna Polarization Loss:	-1.5 dB
Path Loss:	-190.0 dB
Atmospheric Loss:	0 dB
Isotropic Signal Level at Spacecraft:	-146.4 dBm
2nd Spacecraft:	
2nd Spacecraft Antenna Pointing Loss:	0.0 dB
2nd Spacecraft Antenna Gain:	8.3 dBiC
2nd Spacecraft Transmission Line Losses:	-1 dB
S/C Transmission Line Coefficient:	0.7943
2nd Spacecraft Effective Noise Temperature:	250 K
2nd Spacecraft Figure of Merit (G/T):	-16.7 dB/K
S/C Signal-to-Noise Power Density (S/No):	65.5 dBHz
System Desired Data Rate:	1.00×10^7 bps
	50.0 dBHz
System Required Eb/No:	10 dB
System Link Margin:	**5.5 dB**

- *AIAA/ASME/ASCE/AHS/ASC Structures, Structural Dynamics and Materials Conference*, vol. 7, pp. 6662–6674, 2007.

[11] K. G. Klein, O. Alexandrova, J. Bookbinder, D. Caprioli, A. W. Case, B. D. G. Chandran, L. J. Chen, T. Horbury, L. Jian, J. C. Kasper, O. L. Contel, B. A. Maruca, W. Matthaeus, A. Retino, O. Roberts, A. Schekochihin, R. Skoug, C. Smith, J. Steinberg, H. Spence, B. Vasquez, J. M. TenBarge, D. Verscharen, and P. Whittlesey, "Multipoint Measurements of the Solar Wind: A Proposed Advance for Studying Magnetized Turbulence," 2019. [Online]. Available: http://arxiv.org/abs/1903.05740

[12] L. Guan and L. Kepko, "Magnetospheric Constellation: Tracing the flow of mass and energy from the solar wind through the magnetosphere," pp. 1–8. [Online]. Available: http://www8.nationalacademies.org/SSBSurvey/DetailFileDisplay.aspx?id=746&

[13] National Research Council, *Solar and Space Physics: A Science for a Technological Society*. Washington, D.C.: National Academies Press, aug 2013. [Online]. Available: http://www.nap.edu/catalog/13060

[14] National Academy of Sciences, *Achieving Science with CubeSats: Thinking Inside the Box*. Washington, D.C.: National Academies Press, oct 2016. [Online]. Available: https://www.nap.edu/catalog/23503

[15] Y. Zhai, S. A. Cummer, J. L. Green, B. W. Reinisch, M. L. Kaiser, M. J. Reiner, and K. Goetz, "Magnetospheric radio tomographic imaging with IMAGE and Wind," *Journal of Geophysical Research: Space Physics*, vol. 116, no. 12, pp. 1–8, 2011.

[16] V. Angelopoulos, "The THEMIS mission," *Space Science Reviews*, vol. 141, no. 1-4, pp. 5–34, 2008.

[17] NASA Science and Technology Definition Team for the Magnetospheric Constellation Mission, "The Magnetospheric Constellation (MC)," NASA, Tech. Rep., 2004. [Online]. Available: http://stp.gsfc.nasa.gov/missions/

[18] W. Matthaeus, "The essential role of multi-point measurements in turbulence investigations: the solar wind beyond single scale and beyond the Taylor Hypothesis," Tech. Rep. February 2019, 2019.

[19] R. E. Ergun, D. E. Larson, T. Phan, D. Taylor, S. Bale, C. W. Carlson, I. Roth, V. Angelopoulos, J. Raeder, T. Bell, U. S. Inan, J.-L. Bougeret, and R. Manning, "Feasibility of a multisatellite investigation of the Earth's magnetosphere with radio tomography," *Journal of Geophysical Research: Space Physics*, vol. 105, no. A1, pp. 361–373, 2000.

[20] J. Etcheto, Y. De Javel, and M. Petit, "The ISEE Electron Density Experiment," *IEEE Transactions on Geoscience Electronics*, vol. 16, no. 3, pp. 231–238, 1978.

[21] R. Leitinger, "Data from orbiting navigation satellites for tomographic reconstruction," *International Journal of Imaging Systems and Technology*, vol. 5, no. 2, pp. 86–96, 1994.

[22] K. Davies, *Ionospheric radio*, ser. {IEE} electromagnetic waves series. London: P. Peregrinus on behalf of the Institution of Electrical Engineers, 1989, no. v. 31.

[23] M. I. Desai, F. Allegrini, R. W. Ebert, K. Ogasawara, M. E. Epperly, D. E. George, E. R. Christian, S. G. Kanekal, N. Murphy, and B. Randol, "The CubeSat Mission to Study Solar Particles," *IEEE Aerospace and Electronic Systems Magazine*, vol. 34, no. 4, pp. 16–28, 2019.

[24] SpaceX, "Falcon 9," https://www.spacex.com/vehicles/falcon-9/, accessed 2020-09-28.

[25] J. Goodwin and P. Wegner, *Evolved expendable launch vehicle secondary payload adapter - Helping technology get to space*. [Online]. Available: https://arc.aiaa.org/doi/abs/10.2514/6.2001-4701

[26] P. M. Wegner, J. Ganley, and J. R. Maly, "Eelv secondary payload adapter (espa): providing increased access to space," in *2001 IEEE Aerospace Conference Proceedings (Cat. No. 01TH8542)*, vol. 5. IEEE, 2001, pp. 2563–2568.

[27] J. Maly, G. Sanford, A. Williams, and L. Berenberg, "Espa class redefined," in *Proceedings of the AIAA/USU Conference on Small Satellites*, 2017, pp. SSC17–IV.

[28] Y. Miyazaki, "Deployable Techniques for Small Satellites," *Proceedings of the IEEE*, vol. 106, no. 3, pp. 471–483, mar 2018. [Online]. Available: http://ieeexplore.ieee.org/document/8293792/

[29] F. Barao, "Ams—alpha magnetic spectrometer on the international space station," *Nuclear Instruments and Methods in Physics Research Section A: Accelerators, Spectrometers, Detectors and Associated Equipment*, vol. 535, no. 1-2, pp. 134–138, 2004.

[30] R. T. Rajan, R.-v. Schaijk, A. Das, J. Romme, and F. Pasveer, "Reference-Free Calibration in Sensor Networks," *IEEE Sensors Letters*, vol. 2, no. 3, pp. 1–4, 2018.

[31] L. Balzano and R. Nowak, "Blind calibration of sensor networks," *Proceedings of the 6th international conference on Information processing in sensor networks - IPSN '07*, p. 79, 2007. [Online]. Available: http://portal.acm.org/citation.cfm?doid=1236360.1236372

[32] Y. Wang, S. Member, A. Yang, X. Chen, P. Wang, Y. Wang, S. Member, H. Yang, and S. Member, "A Deep Learning Approach for Blind Drift Calibration of Sensor Networks," *IEEE Sensors Journal*, vol. 13, pp. 1558–1748, 2017.

[33] B. Sundararaman, U. Buy, and A. D. Kshemkalyani, "Clock synchronization for wireless sensor networks: a survey," *Ad Hoc Networks*, vol. 3, no. 3, pp. 281–323, may 2005. [Online]. Available: https://linkinghub.elsevier.com/retrieve/pii/S1570870505000144

[34] R. T. Rajan, M. Bentum, and A.-J. Boonstra, "Synchronization for space based ultra low frequency interferometry," in *2013 IEEE Aerospace Conference*. IEEE, mar 2013, pp. 1–8. [Online]. Available: http://ieeexplore.ieee.org/document/6496931/

[35] D. W. Allan, "Statistics of Atomic Frequency Standards," *Proceedings of the IEEE*, vol. 54, no. 2, pp. 221–230, 1966.

[36] Silicon Labs, "Si570/Si571 10 MHZ TO 1.4 GHZ I 2 C PROGRAMMABLE XO/VCXO Features Applications Description," pp. 1–36, 2018. [Online]. Available: https://www.silabs.com/documents/public/data-sheets/si570.pdf

[37] R. T. Rajan and A.-J. van der Veen, "Joint Ranging and Synchronization for an Anchorless Network of Mobile Nodes," *IEEE Transactions on Signal Processing*, vol. 63, no. 8, pp. 1925–1940, apr 2015. [Online]. Available: http://ieeexplore.ieee.org/document/7006748/

[38] M. Kaufmann, A. Tuysuz, J. W. Kolar, and C. Zwyssig, "High-speed magnetically levitated reaction wheels for small satellites," *2016 International Symposium on Power Electronics, Electrical Drives, Automation and Motion, SPEEDAM 2016*, no. Speedam, pp. 28–33, 2016.

[39] S. S. Nudehi, U. Farooq, A. Alasty, and J. Issa, "Satellite attitude control using three reaction wheels," *Proceedings of the American Control Conference*, pp. 4850–4855, 2008.

[40] Blue Canyon Tech., "RWP015 (MicroWheel)," https://storage.googleapis.com/blue-canyon-tech-news/1/2020/06/BCT_DataSheet_Components_ReactionWheels_06_2020.pdf, accessed 2020-09-28.

[41] T. Inamori and S. Nakasuk, *Application of Magnetic Sensors to Nano and Micro-Satellite Attitude Control Systems*, 2012.

[42] ISISpace, "Magnetorquer Board (iMTQ)," https://www.isispace.nl/product/isis-magnetorquer-board/, accessed 2020-09-28.

[43] Blue Canyon Tech., "Standard NST," https://storage.googleapis.com/blue-canyon-tech-news/1/2020/06/BCT_DataSheet_Components_StarTrackers_06_2020.pdf, accessed 2020-09-28.

[44] NewSpace Systems (NSS), "NFSS-411 Sun sensor," https://www.cubesatshop.com/product/digital-fine-sun-sensor/, accessed 2020-09-28.

[45] Sensonor, "STIM377H Inertial Measurement Unit," https://www.sensonor.com/products/inertial-measurement-units/stim377h/, accessed 2020-09-28.

[46] J. Huff, A. Schultz, and M. U. de Haag, "Assured relative and absolute navigation of a swarm of small uas," in *2017 IEEE/AIAA 36th Digital Avionics Systems Conference (DASC)*, 2017, pp. 1–10.

[47] NovAtel, "OEM719 Multi-Frequency GNSS Receiver," https://www.gnssystems.se/kopia-pa-span-igm-s1-gnss-ins-recei, accessed 2020-09-28.

[48] I. Borg, P. J. F. Groenen, and P. Mair, *Applied Multidimensional Scaling*, 2013. [Online]. Available: http://link.springer.com/10.1007/978-3-642-31848-1

[49] B.-H. Lee, K.-H. Oh, T. Hatanaka, and H.-S. Ahn, "Distributed estimation of both position and orientation for networked systems on the sphere," in *2018 Annual IEEE International Systems Conference (SysCon)*. IEEE, apr 2018, pp. 1–6. [Online]. Available: https://ieeexplore.ieee.org/document/8369505/

[50] R. T. Rajan, G. Leus, and A. J. van der Veen, "Relative kinematics of an anchorless network," *Signal Processing*, vol. 157, pp. 266–279, 2019. [Online]. Available: https://doi.org/10.1016/j.sigpro.2018.11.005

[51] I. Levchenko, M. Keidar, J. Cantrell, Y.-L. Wu, H. Kuninaka, K. Bazaka, and S. Xu, "Explore space using swarms of tiny satellites," pp. 185–187, 2018.

[52] A. Freimann, M. Rummelhagen, F. Reichel, M. Marszalek, M. Schmidt, and K. Schilling, "Analysis of wireless networks for satellite swarm missions," *IFAC Proceedings Volumes*, vol. 46, no. 29, pp. 68–73, 2013.

[53] C. Caini, H. Cruickshank, S. Farrell, and M. Marchese, "Delay-and disruption-tolerant networking (dtn): an alternative solution for future satellite networking applications," *Proceedings of the IEEE*, vol. 99, no. 11, pp. 1980–1997, 2011.

[54] D. Burlyaev, "System-level Fault-Tolerance Analysis of Small Satellite On-Board Computers," p. 142, 2012.

[55] A. Keys and M. Watson, "Radiation Hardened Electronics for Extreme Environments," Tech. Rep., 2008. [Online]. Available: https://ntrs.nasa.gov/archive/nasa/casi.ntrs.nasa.gov/20070018806.pdf

[56] P. J. Botma, "The Design and Development of an ADCS OBC for a CubeSat," Ph.D. dissertation, 2011. [Online]. Available: http://scholar.sun.ac.za/handle/10019.1/18040

[57] W. Truszkowski, M. Hinchey, J. Rash, and C. Rouff, "NASA's swarm missions: The challenge of building autonomous software," *IT Professional*, vol. 6, no. 5, pp. 47–52, 2004.

[58] E. E. Alves, D. Bhatt, B. Hall, K. Driscoll, A. Murugesan, and J. Rushby, "Considerations in assuring safety of increasingly autonomous systems," 2018.

[59] J. Cockrell, R. Alena, D. Mayer, H. Sanchez, T. Luzod, B. Yost, and D. M. Klumpar, "EDSN: A Large Swarm of Advanced Yet Very Affordable, COTS-based NanoSats that Enable Multipoint Physics and Open Source Apps," Tech. Rep., 2012. [Online]. Available: https://digitalcommons.usu.edu/smallsat/2012/all2012/89/

[60] A. Babuscia, K. M. Cheung, D. Divsalar, and C. Lee, "Development of cooperative communication techniques for a network of small satellites and CubeSats in deep space: The SOLARA/SARA test case," *Acta Astronautica*, vol. 115, pp. 349–355, 2015. [Online]. Available: http://dx.doi.org/10.1016/j.actaastro.2015.06.001

[61] Azur Space, "32% Quadruple Junction GaAs Solar Cell," p. 2, 2019. [Online]. Available: http://www.azurspace.com/images/0005979-01-00{_}DB{_}4G32C{_}Advanced.pdf

[62] Z. Xiong, Y. S. Yun, and H. J. Jin, "Applications of carbon nanotubes for lithium ion battery anodes," *Materials*, vol. 6, no. 3, pp. 1138–1158, 2013.

[63] Koka, C. Madhusudhana, J. Kishore, and Mourya, "Implementation of Integrated Array Controller and Battery Charger for Small Satellites," *International Journal of Science and Research (IJSR)*, vol. 5, no. 9, pp. 1083–1087, 2016. [Online]. Available: https://www.ijsr.net/archive/v5i9/ART20161414.pdf

[64] B. Glass, "Performance Comparison : Solid State Power Controllers vs . Electromechanical Switching," no. July, 2010.

[65] NASA, "State of the Art of Small Spacecraft Technology," 2019. [Online]. Available: https://sst-soa.arc.nasa.gov/04-propulsion

[66] A. Elwood, R. Burton, R. Carlino, G. Defouw, A. Dono Perez, A. G. Karacalioglu, B. Klamm, A. Rademacher, J. Schalkwyk, R. Shimmin, J. Tilles, and S. Weston, "State of the Art of Small Spacecraft Technology," *State of the Art of Small Spacecraft Technology*, no. December, pp. 114–124, 2018. [Online]. Available: https://sst-soa.arc.nasa.gov/04-propulsion

[67] D. Spence, E. Ehrbar, N. Rosenbald, N. Demmons, T. Roy, S. Hoffman, W. D. Williams, M. Tsay, J. Zwahlen, K. Hohman, V. Hruby, and C. Tocci, "Electrospray Propulsion Systems for Small Satellites and Satlets," 2013.

[68] C. Woodruff, D. King, R. Burton, J. Bowman, and D. Carroll, "Development of a Fiber-Fed Pulsed Plasma Thruster for Small Satellites," pp. 6–11.

[69] C. L. Stevens, "Design, Analysis, Fabrication, and Testing of a Nanosatellite Structure," 2002.

[70] House Select Committee on Astronautics and Space Exploration, "National aeronautics and space act of 1958," p. 13, 1958. [Online]. Available: http://history.nasa.gov/spaceact.html

[71] Assurance, O. of S. and M., "NASA procedural requirements for limiting orbital debris and evaluating the meteoroid and orbital debris environment," p. 1576–1580, 2017.

[72] NASA, "NASA's organization of spectrum management," 2017. [Online]. Available: https://www.nasa.gov/directorates/heo/scan/spectrum/txt_accordion1.html

[73] C. J. Newman and M. Williamson, "Space Sustainability: Reframing the Debate," *Space Policy*, vol. 46, pp. 30–37, nov 2018.

[74] O. Kodheli, E. Lagunas, N. Maturo, S. K. Sharma, B. Shankar, J. Montoya, J. Duncan, D. Spano, S. Chatzinotas, S. Kisseleff *et al.*, "Satellite communications in the new space era: A survey and future challenges," *arXiv preprint arXiv:2002.08811*, 2020.

[75] T. G. Reid, B. Chan, A. Goel, K. Gunning, B. Manning, J. Martin, A. Neish, A. Perkins, and P. Tarantino, "Satellite navigation for the age of autonomy," in *2020 IEEE/ION Position, Location and Navigation Symposium (PLANS)*. IEEE, 2020, pp. 342–352.

[76] D. Krupke, V. Schaus, A. Haas, M. Perk, J. Dippel, B. Grzesik, M. K. B. Larbi, E. Stoll, T. Haylock, H. Konstanski *et al.*, "Automated data retrieval from large-scale distributed satellite systems," in *2019 IEEE 15th International Conference on Automation Science and Engineering (CASE)*. IEEE, 2019, pp. 1789–1795.

[77] Vedant, "Reinforcement learning for spacecraft attitude control," in *70th International Astronautical Congress*, 2019.

[78] B. Bernhard, C. Choi, A. Rahmani, S.-J. Chung, and F. Hadaegh, "Coordinated motion planning for on-orbit satellite inspection using a swarm of small-spacecraft," in *2020 IEEE Aerospace Conference*. IEEE, 2020, pp. 1–13.

[79] S.-H. Mok, J. Guo, E. Gill, and R. T. Rajan, "Autonomous Mission Planning for OLFAR: A Satellite Swarm in Lunar Orbit for Radio Astronomy," in *71th International Astronautical Congress*, 2020.

[80] A. Dono, L. Plice, J. Mueting, T. Conn, and M. Ho, "Propulsion trade studies for spacecraft swarm mission design," in *2018 IEEE Aerospace Conference*. IEEE, 2018, pp. 1–12.